Liberté • Égalité • Fraternité
RÉPUBLIQUE FRANÇAISE

MINISTÈRE
DE L'ÉDUCATION
NATIONALE, DE
L'ENSEIGNEMENT
SUPÉRIEUR ET DE
LA RECHERCHE

EAD BIO 2

SESSION 2017

# AGREGATION
# CONCOURS EXTERNE

## Section : BIOCHIMIE - GÉNIE BIOLOGIQUE

## ÉTUDE DE DOSSIER SCIENTIFIQUE ET TECHNOLOGIQUE

Durée : 4 heures

*L'usage du dictionnaire anglais-français est autorisé.*
*L'usage de tout ouvrage de référence, de tout autre dictionnaire et de tout matériel électronique (y compris la calculatrice) est rigoureusement interdit.*

*Dans le cas où un(e) candidat(e) repère ce qui lui semble être une erreur d'énoncé, il (elle) le signale très lisiblement sur sa copie, propose la correction et poursuit l'épreuve en conséquence.*

*De même, si cela vous conduit à formuler une ou plusieurs hypothèses, il vous est demandé de la (ou les) mentionner explicitement.*

**NB :** ***La copie que vous rendrez ne devra, conformément au principe d'anonymat, comporter aucun signe distinctif, tel que nom, signature, origine, etc. Si le travail qui vous est demandé comporte notamment la rédaction d'un projet ou d'une note, vous devrez impérativement vous abstenir de signer ou de l'identifier.***

# Un nouvel organisme modèle pour l'étude de l'autophagie

La macroautophagie, souvent appelée autophagie, est un processus au cours duquel la cellule eucaryote dégrade et recycle des éléments cytoplasmiques (organites, constituants cytosoliques…). Il s'agit d'une fonction cellulaire fondamentale et très conservée chez les *Eucaryotes*.

A l'aide des articles proposés dans le dossier technique et en lien avec le contexte de l'étude, présenter le travail de recherche, tant dans sa dimension scientifique que dans ses aspects technologiques, et ses conséquences sur la santé. Lors de la composition, il sera apprécié la critique et la mise en perspective pédagogique des travaux présentés en lien avec les connaissances générales abordées au niveau bac + 2.

**Le dossier technique comporte deux parties :**

**Revue :** **Autophagy as a regulated pathway of cellular degradation**

Daniel J. Klionsky and Scott D. Emr
*Science,* 2000, vol. 290, p. 1717-1721

**Publication :** **The thermotolerant yeast *Kluyveromyces marxianus* is a useful organism for structural and biochemical studies of autophagy**

Hayashi Yamamoto, Takayuki Shima, Masaya Yamaguchi, Yuh Mochizuki, Hisashi Hoshida, Soichiro Kakuta, Chika Kondo-Kakuta, Nobuo N. Noda, Fuyuhiko Inagaki, Takehiko Itoh, Rinji Akada, and Yoshinori Ohsumi
*The Journal of Biological Chemistry*, 2015, vol. 290, p. 29506-29518

SCIENCE'S COMPASS • REVIEW

REVIEW: CELL BIOLOGY

# Autophagy as a Regulated Pathway of Cellular Degradation

Daniel J. Klionsky[1]* and Scott D. Emr[2]

**Macroautophagy is a dynamic process involving the rearrangement of subcellular membranes to sequester cytoplasm and organelles for delivery to the lysosome or vacuole where the sequestered cargo is degraded and recycled. This process takes place in all eukaryotic cells. It is highly regulated through the action of various kinases, phosphatases, and guanosine triphosphatases (GTPases). The core protein machinery that is necessary to drive formation and consumption of intermediates in the macroautophagy pathway includes a ubiquitin-like protein conjugation system and a protein complex that directs membrane docking and fusion at the lysosome or vacuole. Macroautophagy plays an important role in developmental processes, human disease, and cellular response to nutrient deprivation.**

Normal cell growth and development requires a well-controlled balance between protein synthesis and organelle biogenesis versus protein degradation and organelle turnover. The major pathways for degradation of cellular constituents are autophagy and cytosolic turnover by the proteasome. These degradative pathways are particularly important during development and under certain environmental stress conditions. For example, cellular death and resorption are critical during processes that involve extensive cellular remodeling such as insect metamorphosis, postpartum luteal cell regression, differentiation, and aging (*1*, *2*), as well as in preventing various disease states including cardiomyopathy and some types of cancer. In some cases, degradation and turnover of the entire cell occurs as part of programmed cell death. At other times, turnover occurs on a subcellular scale; under starvation conditions, cells need to scavenge nonessential proteins and organelles and to recycle the components for reuse in the cytosol.

In eukaryotic cells, the lysosome or vacuole is a major degradative organelle. This compartment contains a range of hydrolases that are able to degrade essentially any subcellular constituent (proteins, lipids, nucleic acids, and carbohydrates). In addition, regulated turnover of organelles is confined to the lysosome. Cytoplasmic components are degraded within the lysosome by microautophagy, chaperone-mediated autophagy, and macroautophagy (*3*–*5*). In mammalian cells, microautophagy has not been well characterized, and chaperone-mediated autophagy is a secondary response that temporally follows macroautophagy. In this review, we will limit our discussion to macroautophagy, the major inducible pathway for general turnover of cytoplasmic components. The process of macroautophagy is seen in all nucleate cell types that have been analyzed. The morphology of the process is essentially the same in yeast, plants, and animal cells. In addition, the recent identification of genes encoding components of the autophagic machinery in several organisms indicates that the autophagic process is highly conserved.

## Morphology, Biochemistry, and Genetics

Macroautophagy is a dynamic process in which subcellular membranes undergo dramatic morphological changes [for reviews, see (*5*, *6*)]. In this process, portions of cytoplasm are sequestered within double-membrane vesicles known as autophagic vacuoles in mammalian cells or autophagosomes in yeast (Fig. 1). For simplicity, we will use the term autophagosome. Macroautophagy has been extensively characterized morphologically in both yeast and mammalian systems. Genetic screens have been used in yeast to identify the genes that are involved in the autophagic process (Table 1). Screens for yeast mutants that were starvation-sensitive or defective in the degradation of specific cytosolic proteins (*7*, *8*) produced *apg* and *aut* mutants, which overlap with mutants in the cytoplasm to vacuole targeting (Cvt) pathway, that were isolated because of defects in proteolytic processing of the resident vacuolar hydrolase aminopeptidase I (*9*–*11*). The overlap between the *apg*, *aut*, and *cvt* mutants was surprising, because the respective pathways, autophagy and Cvt, operate under distinct conditions. Autophagy is primarily used for degradation and is induced under starvation conditions. In contrast, the Cvt pathway is biosynthetic and operates under nutrient-rich conditions. However, biochemical and morphological studies show that in both pathways, the basic mechanism of cytoplasm-to-vacuole transport involves sequestration by a cytosolic double-membrane vesicle (*12*, *13*). The major distinction between the two pathways appears to be the regulation of the size of the autophagosome. The process of macroautophagy can be broken down into at least four discrete steps: induction, formation of the autophagosome, autophagosome docking and fusion with the lysosome or vacuole, and autophagic body breakdown. The molecular details of these steps have begun to be elucidated.

*Induction of macroautophagy*. Autophagic degradation is both developmentally and nutritionally regulated. Nonspecific autophagy is inhibited under nutrient-rich conditions and is induced by starvation. In mammalian cells, phosphorylation of ribosomal protein S6 strongly correlates with inhibition of macroautophagy (*14*). The activity of p70S6 kinase is regulated by mTor kinase (*15*, *16*). Inhibition of phosphorylation resulting from inactivation of mTor by treatment with rapamycin induces autophagy even under nutrient-rich conditions; however, the details of the regulatory mechanism are not understood. As in mammalian cells, autophagy can be induced in yeast by rapamycin-dependent inhibition of Tor2 (*17*). In yeast, Tor2 phosphorylates Tap42 causing it to interact with protein phosphatase 2A (PP2A), resulting in a decrease in PP2A activity (*18*). Inhibition of Tor2 results in activation of PP2A and the induction of autophagy. In mammalian cells, inhibition of PP2A by okadaic acid has a strong inhibitory effect on autophagy (*19*). Thus, changes in localization and/or activity of PP2A may be one mechanism that controls autophagy, although other phosphatases are also involved in its regulation (*20*).

Although Tor2 regulates the expression of many genes, the majority of *APG* genes are constitutively expressed. In part, this is owing to the overlap between autophagy and the biosynthetic Cvt pathway. Accordingly, it appears that Tor2 may regulate the transition from the Cvt pathway to autophagy during the response

[1]Department of Biology, University of Michigan, 830 North University, Ann Arbor, MI 48109–1048, USA. [2]Division of Cellular and Molecular Medicine, University of California, San Diego, School of Medicine, and Howard Hughes Medical Institute, La Jolla, CA 92093–0668, USA.

*To whom correspondence should be addressed. E-mail: klionsky@umich.edu

to starvation. One of the downstream effectors of the yeast Tor2 kinase may be the Apg13 protein (Fig. 2). Apg13 is part of a dynamic protein complex, which includes the serine and threonine kinase Apg1 (*20*, *21*). Under nutrient-rich conditions, Apg13 is highly phosphorylated and maintains a weak interaction with the Apg1 kinase. Upon inhibition of the Tor2 kinase, and presumably activation of a phosphatase, Apg13 is partially dephosphorylated and associates more tightly with Apg1, stimulating its kinase activity (Fig. 2). Thus, the Apg1 kinase appears to act downstream of Apg13; however, its target or targets have not been identified. The Apg1 kinase interacts with at least two other proteins, Apg17 and Cvt9. These two proteins have specific functions in either the autophagic or Cvt pathways, respectively (*20*). This finding fits well with the predicted role of the Apg13-Apg1 complex in controlling transition between biosynthetic and degradative pathways. The identification of *APG1* homologs in *Caenorhabditis elegans* (*22*) and mice (*23*) suggests that the Apg1 kinase is required for autophagy in higher eukaryotes.

*Formation of the autophagosome*. After induction of autophagy, a double-membrane vesicle begins to form in the cytosol, resulting in the sequestration of cytoplasmic components (Fig. 1). The origin of the sequestering membrane is not known, but for mammalian cells, it is generally thought to be the endoplasmic reticulum (*24*). However, an alternative compartment termed the phagophore may represent the donor membrane (*25*). Sequestration is highly regulated and is under the control of GTPases, phosphatidylinositol kinases, and various phosphatases. Increasing the levels of the class III phosphoinositide 3-kinase product phosphatidylinositol 3-phosphate in human colon cancer cells stimulates macroautophagy (*26*). In contrast, increases in class I phosphoinositide 3-kinase products, phosphatidylinositol 3,4-bisphosphate and phosphatidylinositol 3,4,5-trisphosphate, inhibit autophagy (*26*). In addition, the guanosine diphosphate (GDP)–bound form of the heterotrimeric G protein subunit $G\alpha_{i3}$ is an activating factor for autophagy, whereas the GTP-bound form is inhibitory (*27*). Regulation by protein phosphatases and kinases is complex and not yet resolved (*28*).

Molecular genetic studies in yeast have identified some of the components required for autophagosome formation. The sequestration process involves a protein conjugation system (*29*) (Fig. 2). Apg12 is covalently attached to Apg5 through a COOH-terminal glycine and an internal lysine residue, respectively. This process requires the action of the Apg7 protein, which is homologous to the E1 family of ubiquitin-activating enzymes (*30*, *31*), and Apg10, which functions as a protein-conjugating enzyme (*32*). A third protein, Apg16, binds to the conjugated Apg5 and dimerizes to link a pair of Apg12-Apg5 conjugates (*33*). This conjugation event is required for formation or completion of the sequestering vesicle (*34*). Human homologs of Apg5 and Apg12 have been identified and undergo a similar covalent linkage, indicating that this conjugation system is conserved in mammalian cells (*35*).

The level of most proteins involved in autophagy does not change during a shift from nutrient-rich to starvation conditions. In contrast, the *AUT7* gene is highly up-regulated under starvation conditions or after rapamycin treatment (*36*, *37*) (Fig. 2). Aut7 binds the forming autophagosome and becomes sequestered inside the vesicle along with the cytoplasmic cargo. The localization and up-regulation of Aut7 suggests that it functions at least in part as a structural component during autophagosome formation.

*Autophagosome docking and fusion*. In mammalian cells, delivery to and fusion of the completed autophagosome with the lysosome (Fig. 1) depends on microtubules and maintenance of proper acidification. In yeast, components of the SNARE machinery, including the vacuolar syntaxin homolog Vam3p (*38*) and the SNAP-25 homolog Vam7p (*39*), are required for autophagosome docking and/or fusion with the vacuole (Table 1). In addition, the regulatory Rab GTPase, Ypt7 (*30*), and the class C Vps protein complex (*13*, *40*–*42*) also function at this step to ensure the accurate and efficient fusion of the autophagosome with the vacuole.

*Autophagic body breakdown*. Although the lysosome or vacuole is the terminal destination for endocytic and certain biosynthetic trafficking pathways, little is known about what happens to membranes after their delivery to this organelle. After fusion of the autophagosome with the vacuole, the outer membrane of the autophagosome is incorporated into the limiting membrane of the vacuole (Fig. 1). It is not known how this large patch of new membrane avoids degradation by the lipases and other hydrolases present within this organelle. The vacuole membrane itself contains a variety of glycoproteins that are presumed to play a role in protecting this membrane from degradation. Fusion causes the release of the single-membrane bound inner vesicle of the autophagosome, the autophagic body (Fig. 1), into the vacuole lumen. Because of the degradative nature of the lysosome or vacuole, the autophagic body is broken down. Efficient degradation is dependent on proteinase B, lumenal acidification, and the Cvt17 protein, a candidate lipase that may degrade the autophagic body (*13*, *43*–*45*).

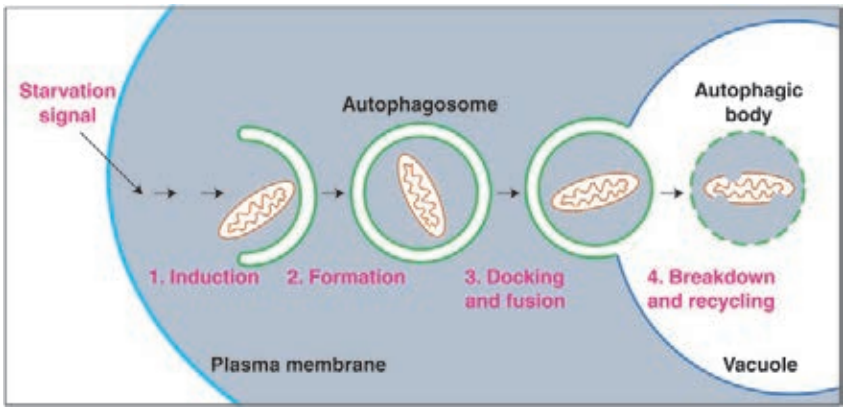


**Fig. 1.** Schematic model of macroautophagy in yeast. A signal transduction event regulated by the Tor kinase leads to the following: (1) The induction of autophagy. (2) Membrane from an unknown source sequesters cytosol and/or organelles (a mitochondrion is depicted) resulting in the formation of a double-membrane vesicle (300 to 900 nm) termed an autophagosome. (3) On completion, the autophagosome docks with the lysosome or vacuole. Fusion of the autophagosome outer membrane with the vacuole releases the inner vesicle into the vacuole lumen. The inner vesicle is termed an autophagic body. (4) Breakdown within the vacuole allows recycling of the degraded autophagic body and its hydrolyzed cargo (amino acids, fatty acids, sugars, and nucleotides). The morphology of macroautophagy in mammalian cells is similar to that shown; however, in mammalian cells autophagy can be induced by environmental cues other than starvation.

## Specific Autophagic Pathways

*Biosynthetic transport and organelle turnover*. Autophagy is a ubiquitous process that occurs in plant, animal, and fungal cells. Although autophagy is generally considered to be nonselective, the protein components required for autophagic uptake are also used in specific transport events. For example, as noted above, autophagy in yeast overlaps with the biosynthetic Cvt pathway that transports aminopeptidase I (API) to the vacuole. API is synthesized as a precursor in the cytosol and rapidly oligomerizes into a dodecamer (*46*). The dodecameric precursor API assembles into a larger complex composed of multiple dodecamers, termed a Cvt complex. The Cvt complex is then enwrapped by a double-membrane that forms a cytosolic vesicle. This Cvt vesicle is smaller than an autophagosome and appears to exclude cytosol

(*12*, *13*). After fusion with the vacuole, the inner vesicle is degraded in the lumen, allowing release and maturation of precursor API.

In addition to the biosynthetic transport of precursor API, regulated autophagy functions in the selective sorting and turnover of certain cytoplasmic organelles. When methylotrophic yeasts or mammalian cells are grown on methanol or fatty acids, respectively, peroxisomes proliferate to allow maximal use of the available nutrients. Adaptation to preferred carbon sources such as glucose or ethanol result in the specific degradation of peroxisomes through an autophagic mechanism termed pexophagy (*5*). In some yeasts this degradation has been shown to occur by both micropexophagy, occurring at the vacuole surface, and macropexophagy, where the initial sequestration step takes place away from the vacuole (*47*). The proteins required for macroautophagy are also required for pexophagy (*48*, *49*).

In general, maintenance of organelles is energetically costly. Organelles like the peroxisome are specifically degraded when they are no longer needed. In mitochondria, certain types of stress can lead to a loss of integrity of the inner and outer membranes resulting in depolarization, a process termed the "mitochondrial permeability transition" (*50*). It has been proposed that conversion of the mitochondrial permeability transition pore to an open state leads to mitochondrial degradation through macroautophagy and subsequently through apoptosis and necrosis (*51*). Macroautophagy then can protect cells from oxidative damage that could result from a loss of mitochondrial integrity without triggering apoptosis. However, lysosomal degradation of mitochondria can lead to clinical problems in patients lacking one or more lysosomal hydrolases. The lysosomal accumulation of subunit 9 of the mitochondrial ATPase due to inefficient degradation is associated with neuronal ceroid lipofuscinosis (Batten disease), a neurodegenerative disorder in children and young adults (*52*). In yeast, mitochondria have been detected within autophagosomes (*43*), providing additional evidence for mitochondrial degradation by macroautophagy.

*Autophagy in development and disease.* Macroautophagy plays a critical role in the homeostatic process of recycling proteins and organelles. However, autophagy has also been linked to developmental and pathological conditions. For example, intersegmental muscles are required in the larval and pupal stages of the moth life cycle and during emergence of the adult moth. These muscle cells are not needed in the adult and undergo cell death shortly after emergence. In this case, the characteristics of cell death are largely distinct from those associated with apoptosis and are proposed to occur through autophagy (*53*). Programmed cell death in developing neurons clearly involves apoptosis (*54*). However, cellular death in neurons may also involve autophagy (*55*, *56*). Similarly, the loss of Rohon-Beard neurons from the spinal cord of *Xenopus* tadpoles requires the activity of lysosomal hydrolases and is thought to occur through autophagy-related cell death (*57*).

There are many lines of evidence that connect macroautophagy to human disease. For example, elevated levels of autophagy are associated with neurodegenerative diseases such as Parkinson's (*58*). The mechanism by which neuronal degeneration occurs is not well understood and clearly requires further study to allow the development of effective treatments. In contrast to the situation with Parkinson's disease, lowered levels of autophagy are problematic in other diseases. A direct link to autophagy and heart disease was discovered by the finding that a deficiency of LAMP-2, a transmembrane protein in the late endosome and lysosome, is associated with the cardiomyopathic Danon's disease (*59*), and LAMP-2–deficient mice are defective in the maturation of autophagosomes (*60*). Similarly, reduced levels of autophagy are seen in some forms of cancer (*61*). A key role for autophagy in controlling the unregulated cell growth that is associated with tumor development has been suggested through the study of a tumor suppressor gene, *beclin 1* (*62*). *Beclin 1* is the human homolog of the yeast autophagy gene *APG6*. Beclin 1 interacts with the antiapoptotic protein Bcl-2, which prevents the Bax-dependent release of mitochondrial cytochrome c. Decreased levels of the Beclin 1 protein have been correlated with the development or progression of breast tumors. In multicellular organisms, autophagy has also been linked with programmed cell death. Autophagy is specifically associated with type II (nonapoptotic) programmed cell death (*53*, *63*). However, there is an indication that early stages of autophagy may play a role in type I (apoptotic) programmed cell

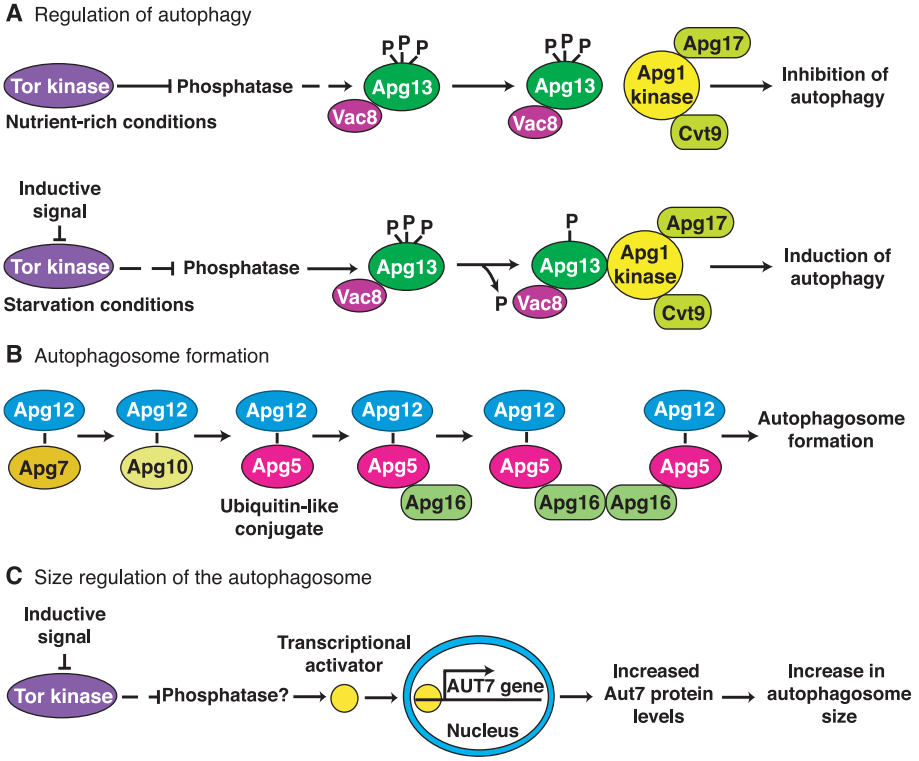


**Fig. 2.** Molecular genetics of macroautophagy in yeast. (**A**) The Tor kinase exerts a negative regulatory effect on autophagy when cells are growing under nutrient-rich conditions. When starvation occurs, the Tor kinase is inactivated, and the negative regulation is relieved resulting in induction of autophagy. Most of the proteins required for autophagy are constitutively expressed and are used for biosynthetic import through the cytoplasm to vacuole targeting pathway under these conditions. The downstream effectors of Tor are likely to include phosphatases and kinases that modulate the phosphorylation state of Apg13. An inductive signal such as carbon or nitrogen starvation inactivates Tor and results in partial dephosphorylation of Apg13. This form of Apg13 associates more tightly with the Apg1 kinase and stimulates its activity. The function of Apg1 kinase is required for autophagosome formation. (**B**) The Apg7 (E1-like) and Apg10 proteins form thioester intermediates through a COOH-terminal glycine of Apg12. Apg12 is ultimately conjugated to Apg5 through an internal lysine residue in Apg5 in a process that is similar to ubiquitination. Apg16 binds the conjugated Apg5 protein noncovalently and dimerizes to form a complex that is required for formation and completion of the autophagosome. (**C**) Under nutrient-rich conditions, the Tor kinase negatively regulates the expression of the *AUT7* gene resulting in basal levels of Aut7 synthesis. Under these conditions the Cvt pathway is operative and 150-nm Cvt vesicles are formed. Inhibition of Tor by transduction of an environmental signal or after treatment with rapamycin allows the activation of a presumed transcriptional activator protein that increases expression of *AUT7*. The resulting increase in Aut7 levels allows an expansion in the size of the autophagosome from 150 nm to a range of 300 to 900 nm.

death (*64*). Along these lines, a human apoptosis-specific protein was shown to be homologous to the *APG5* gene product (*65*). Inhibition of autophagy may be therapeutic in certain neurodegenerative diseases, although its selective activation in specific cells could provide an avenue for cancer treatment.

An interesting connection between apoptosis and autophagy also has been seen in the coordinated regulation of Akt ( protein kinase B) and p70S6 kinase. The activity of p70S6 kinase is controlled through mTor but also through the action of the phosphoinositide-dependent protein kinase–1, PDK1 (*66*, *67*). PDK1 is a multifunctional effector that regulates various kinases (*68*, *69*). Phosphorylation of p70S6 kinase by mTor, or presumably PDK1, prevents autophagy. Class I phosphatidylinositol 3-kinase (PI 3-kinase) activity allows the membrane recruitment of Akt through its pleckstrin homology domain. Phosphorylation by PDK1 activates Akt and inhibits apoptosis (*70*). Thus, class I PI 3-kinase products may block both apoptosis and autophagy through PDK1. Along these lines, some of the same signals that trigger apoptosis may induce autophagy (*55*). Once it is activated, autophagy may be able to cause cell death even in the presence of apoptosis inhibitors. These findings support the idea that autophagy represents a second mechanism for programmed cell death. In fact, autophagy-related programmed cell death may have evolved before apoptosis (*53*).

## Conclusions

The capacity for limited turnover of cytoplasmic contents by autophagy or for the programmed death of specific cells plays an important role in development. However, the capacity to degrade cells and cellular contents necessitates strict regulatory safeguards to prevent indiscriminate destruction of essential components. Accordingly, macroautophagy is regulated through the action of kinases (e.g., Tor and Apg1), phosphatases (e.g., PP2A), and GTPases ($G\alpha_{i3}$ and Ypt7) that dictate the conditions under which it operates and the targets of the sequestration process.

**Table 1.** Genes required for the autophagy and Cvt pathways.

| Gene | Mammalian homolog | Characteristics | References |
|---|---|---|---|
| Induction of autophagy and formation of autophagosome | | | |
| Kinase signaling system | | | |
| *Tor2* | mTor | Rapamycin-sensitive protein kinase | (*15*) |
| *APG1* | *ULK1* | SER or THR protein kinase, in complex with Apg13, Apg17, Cvt9 | (*23*, *44*) |
| *APG6* | *BECN1* | 63-kD peripheral membrane protein, binds Apg14 | (*62*, *71*) |
| *APG9* | | Integral membrane protein | (*72*) |
| *APG13* | | Associates with and activates Apg1 kinase | (*20*) |
| *APG14* | | Peripheral membrane protein, interacts with Apg6 | (*71*) |
| *APG17* | | Interacts with Apg1 kinase, specific for autophagy | (*20*) |
| *CVT9* | | Interacts with Apg1 kinase, specific for Cvt pathway | (*20*) |
| *VAC8* | | Armadillo repeat protein, interacts with Apg13 | (*21*, *73*) |
| APG protein conjugation system | | | |
| *APG5* | *hAPG5* | 34-kD protein that forms conjugate with Apg12 | (*29*) |
| *APG7* | *HsGSA7* | E1-like ubiquitin activating enzyme | (*30*, *31*) |
| *APG10* | | Protein-conjugating enzyme | (*32*) |
| *APG12* | *hAPG12* | Ubiquitin type modifier | (*29*) |
| *APG16* | | Coiled-coil protein that binds Apg5 | (*33*) |
| Size regulation of the autophagosome | | | |
| *AUT2* | | Cysteine protease processes Aut7 | (*74*) |
| *AUT7* | GATE-16 MAP LC3 | Up-regulated by starvation, regulates autophagosome size | (*36*, *37*, *75*–*77*) |
| Docking and fusion | | | |
| *VAM3* | Syntaxin 7 | Vacuolar tSNARE | (*38*, *78*, *79*) |
| *VAM7* | | SNAP-25 family member, forms part of SNARE complex | (*39*) |
| *VPS* genes | | Class C Vps complex composed of Vps11, 16, 18, 33, 39, and 41 | (*41*, *42*) |
| *YPT7* | Rab7 | Rab GTPase | (*80*) |
| Breakdown | | | |
| *CVT17* | | Lipase homolog | (*13*, *45*) |
| *PRB1* | | Vacuolar proteinase | (*43*) |
| *VMA* genes | V-ATPase | Vacuolar-type ATPase acidifies lumen | (*81*, *82*) |

Autophagy involves dynamic rearrangements of cellular membranes. This is not surprising as this process can result in the engulfment of entire organelles. Some aspects of autophagy are similar to those of other subcellular trafficking events, for example, the targeting, docking, and fusion of the autophagosome requires components such as Rabs and SNARES that are used in both the secretory and endocytic transport systems. However, other components of the autophagy system are specific (see Table 1). The origin of the sequestering membrane is not known, nor is it understood how this membrane can form an enwrapping vesicle in the cytosol. Formation of the autophagosome is topologically distinct from that of a transit vesicle that buds off a preexisting organelle and is likely to require a large number of gene products (Table 1), including those of a novel ubiquitin-like protein conjugation system (Fig. 2). The autophagic machinery is used for a range of processes that are carried out under different conditions and that display varying specificities.

The autophagic machinery is highly conserved in organisms as diverse as plants, animals, and yeast. Recent studies have demonstrated a role for autophagy in both promoting and preventing human diseases. In the last few years, tremendous advances have been made in identifying the molecular components required for macroautophagy through genetic studies in yeast. Combining these analyses with the pharmacological and biochemical information that is available from work in mammalian systems has begun to provide a detailed understanding of the mechanisms that underlie each stage of the autophagic process. Furthermore, workers in both plant and animal systems are exploiting the genomic data now available to identify homologs of the yeast *APG* genes for directed studies in these multicellular systems. Such studies should allow researchers to address tissue- and development-specific roles for autophagic degradation. Many questions still remain, including the following: What is the mechanism by which cells sense the starvation signal required to induce autophagy? What is the origin of the autophagosomal membrane? How does the autophagic machinery drive the deformation of membranes? How are specific substrates recognized as cargo for sequestration? However, with the progress that has been made in the last few years, it is likely that these and other important problems in the field of autophagy will be solved in the near future.

### References and Notes


1. G. E. Mortimore, G. Miotto, R. Venerando, M. Kadowaki, *Subcell. Biochem.* **27**, 93 (1996).
2. S. Vittorini *et al.*, *J. Gerontol. A Biol. Sci. Med. Sci.* **54**, B318 (1999).
3. W. A. Dunn Jr., *Trends Cell Biol.* **4**, 139 (1994).
4. A. M. Cuervo, J. F. Dice, *J. Mol. Med.* **76**, 6 (1998).
5. J. Kim, D. J. Klionsky, *Annu. Rev. Biochem.* **69**, 303 (2000).
6. D. J. Klionsky, Y. Ohsumi, *Annu. Rev. Cell. Dev. Biol.* **15**, 1 (1999).

7. M. Thumm *et al.*, *FEBS Lett.* **349**, 275 (1994).
8. M. Tsukada, Y. Ohsumi, *FEBS Lett.* **333**, 169 (1993).
9. T. M. Harding, K. A. Morano, S. V. Scott, D. J. Klionsky, *J. Cell Biol.* **131**, 591 (1995).
10. T. M. Harding, A. Hefner-Gravink, M. Thumm, D. J. Klionsky, *J. Biol. Chem.* **271**, 17621 (1996).
11. S. V. Scott *et al.*, *Proc. Natl. Acad. Sci. U.S.A.* **93**, 12304 (1996).
12. M. Baba, M. Osumi, S. V. Scott, D. J. Klionsky, Y. Ohsumi, *J. Cell Biol.* **139**, 1687 (1997).
13. S. V. Scott, M. Baba, Y. Ohsumi, D. J. Klionsky, *J. Cell Biol.* **138**, 37 (1997).
14. E. F. Blommaart, J. J. Luiken, P. J. Blommaart, G. M. van Woerkom, A. J. Meijer, *J. Biol. Chem.* **270**, 2320 (1995).
15. G. Thomas, M. N. Hall, *Curr. Opin. Cell Biol.* **9**, 782 (1997).
16. E. J. Brown *et al.*, *Nature* **377**, 441 (1995).
17. T. Noda, Y. Ohsumi, *J. Biol. Chem.* **273**, 3963 (1998).
18. T. Beck, M. N. Hall, *Nature* **402**, 689 (1999).
19. I. Holen, P. B. Gordon, P. O. Seglen, *Biochem. J.* **284**, 633 (1992).
20. Y. Kamada *et al.*, *J. Cell Biol.* **150**, 1507 (2000).
21. S. Scott *et al.*, *J. Biol. Chem.* **275**, 25840 (2000).
22. K. Ogura *et al.*, *Genes Dev.* **8**, 2389 (1994).
23. J. Yan *et al.*, *Biochem. Biophys. Res. Commun.* **246**, 222 (1998).
24. W. A. Dunn Jr., *J. Cell Biol.* **110**, 1923 (1990).
25. P. E. Strømhaug, T. O. Berg, M. Fengsrud, P. O. Seglen, *Biochem. J.* **335**, 217 (1998).
26. A. Petiot, E. Ogier-Denis, E. F. Blommaart, A. J. Meijer, P. Codogno, *J. Biol. Chem.* **275**, 992 (2000).
27. E. Ogier-Denis, J.-J. Houri, C. Bauvy, P. Codogno, *J. Biol. Chem.* **271**, 28593 (1996).
28. P. Codogno, E. Ogier-Denis, J.-J. Houri, *Cell. Signal.* **9**, 125 (1997).
29. N. Mizushima *et al.*, *Nature* **395**, 395 (1998).
30. J. Kim, V. M. Dalton, K. P. Eggerton, S. V. Scott, D. J. Klionsky, *Mol. Biol. Cell* **10**, 1337 (1999).
31. I. Tanida *et al.*, *Mol. Biol. Cell* **10**, 1367 (1999).
32. T. Shintani *et al.*, *EMBO J.* **18**, 5234 (1999).
33. N. Mizushima, T. Noda, Y. Ohsumi, *EMBO J.* **18**, 3888 (1999).
34. M. D. George *et al.*, *Mol. Biol. Cell* **11**, 969 (2000).
35. N. Mizushima, H. Sugita, T. Yoshimori, Y. Ohsumi, *J. Biol. Chem.* **273**, 33889 (1998).
36. W. P. Huang, S. V. Scott, J. Kim, D. J. Klionsky, *J. Biol. Chem.* **275**, 5845 (2000).
37. T. Kirisako *et al.*, *J. Cell Biol.* **147**, 435 (1999).
38. T. Darsow, S. E. Rieder, S. D. Emr, *J. Cell Biol.* **138**, 517 (1997).
39. T. K. Sato, T. Darsow, S. D. Emr, *Mol. Cell. Biol.* **18**, 5308 (1998).
40. S. E. Rieder, S. D. Emr, *Mol. Biol. Cell* **8**, 2307 (1997).
41. T. K. Sato, P. Rehling, M. R. Peterson, S. D. Emr, *Mol. Cell* **6**, 661 (2000).
42. D. F. Seals, G. Eitzen, N. Margolis, W. T. Wickner, A. Price, *Proc. Natl. Acad. Sci. U.S.A.* **97**, 9402 (2000).
43. K. Takeshige, M. Baba, S. Tsuboi, T. Noda, Y. Ohsumi, *J. Cell Biol.* **119**, 301 (1992).
44. A. Matsuura, M. Tsukada, Y. Wada, Y. Ohsumi, *Gene* **192**, 245 (1997).
45. S. A. Teter, D. J. Klionsky, unpublished data.
46. J. Kim, S. V. Scott, M. Oda, D. J. Klionsky, *J. Cell Biol.* **137**, 609 (1997).
47. D. L. Tuttle, W. A. Dunn Jr., *J. Cell Sci.* **108**, 25 (1995).
48. W. Yuan, P. E. Stromhaug, W. A. Dunn Jr., *Mol. Biol. Cell* **10**, 1353 (1999).
49. M. U. Hutchins, M. Veenhuis, D. J. Klionsky, *J. Cell Sci.* **112**, 4079 (1999).
50. M. Crompton, *Biochem. J.* **341**, 233 (1999).
51. J. J. Lemasters *et al.*, *Biochim. Biophys. Acta* **1366**, 177 (1998).
52. G. Dawson, S. Cho, *J. Neurosci. Res.* **60**, 133 (2000).
53. L. M. Schwartz, S. W. Smith, M. E. Jones, B. A. Osborne, *Proc. Natl. Acad. Sci. U.S.A.* **90**, 980 (1993).
54. H. Dudek *et al.*, *Science* **275**, 661 (1997).
55. L. Xue, G. C. Fletcher, A. M. Tolkovsky, *Mol. Cell. Neurosci.* **14**, 180 (1999).
56. K. Isahara *et al.*, *Neuroscience* **91**, 233 (1999).
57. J. E. Lamborghini, *J. Comp. Neurol.* **264**, 47 (1987).
58. P. Anglade *et al.*, *Histol. Histopathol.* **12**, 25 (1997).
59. I. Nishino *et al.*, *Nature* **406**, 906 (2000).
60. Y. Tanaka *et al.*, *Nature* **406**, 902 (2000).
61. R. Schulte-Hermann *et al.*, *Toxicol. Pathol.* **25**, 89 (1997).
62. X. H. Liang *et al.*, *Nature* **402**, 672 (1999).
63. W. Bursch *et al.*, *J. Cell Sci.* **113**, 1189 (2000).
64. L. Jia *et al.*, *Br. J. Haematol.* **98**, 673 (1997).
65. E. M. Hammond *et al.*, *FEBS Lett.* **425**, 391 (1998).
66. D. R. Alessi, M. T. Kozlowski, Q. P. Weng, N. Morrice, J. Avruch, *Curr. Biol.* **8**, 69 (1998).
67. N. Pullen *et al.*, *Science* **279**, 707 (1998).
68. B. Vanhaesebroeck, D. R. Alessi, *Biochem. J.* **346**, 561 (2000).
69. P. J. Coffer, J. Jin, J. R. Woodgett, *Biochem. J.* **335**, 1 (1998).
70. B. A. Hemmings, *Science* **275**, 628 (1997).
71. S. Kametaka, T. Okano, M. Ohsumi, Y. Ohsumi, *J. Biol. Chem.* **273**, 22284 (1998).
72. T. Noda *et al.*, *J. Cell Biol.* **148**, 465 (2000).
73. Y. X. Wang, N. L. Catlett, L. S. Weisman, *J. Cell Biol.* **140**, 1063 (1998).
74. T. Kirisako *et al.*, *J. Cell Biol.* **151**, 263 (2000).
75. Y. Sagiv, A. Legesse-Miller, A. Porat, Z. Elazar, *EMBO J.* **19**, 1494 (2000).
76. T. Lang *et al.*, *EMBO J.* **17**, 3597 (1998).
77. Y. Kabeya *et al.*, *EMBO J.* **19**, 5720 (2000).
78. Y. Wada, N. Nakamura, Y. Ohsumi, A. Hirata, *J. Cell Sci.* **110**, 1299 (1997).
79. B. M. Mullock *et al.*, *Mol. Biol. Cell* **11**, 3137 (2000).
80. A. Haas, D. Scheglmann, T. Lazar, D. Gallwitz, W. Wickner, *EMBO J.* **14**, 5258 (1995).
81. L. A. Graham, B. Powell, T. H. Stevens, *J. Exp. Biol.* **203**, 61 (2000).
82. N. Nakamura, A. Matsuura, Y. Wada, Y. Ohsumi, *J. Biochem.* **121**, 338 (1997).

83. The authors would like to thank J. Kim, T. Sato, A. Wurmser, and S. Scott for helpful comments. D.J.K. is supported by Public Health Service grant GM53396 from NIH and S.D.E. is supported by NIH grant CA58689 and is an Investigator with the Howard Hughes Medical Institute.

THE JOURNAL OF BIOLOGICAL CHEMISTRY VOL. 290, NO. 49, pp. 29506–29518, December 4, 2015


# The Thermotolerant Yeast *Kluyveromyces marxianus* Is a Useful Organism for Structural and Biochemical Studies of Autophagy*[S]

Received for publication, August 7, 2015, and in revised form, September 25, 2015 Published, JBC Papers in Press, October 6, 2015, DOI 10.1074/jbc.M115.684233

**Hayashi Yamamoto[‡1], Takayuki Shima[‡], Masaya Yamaguchi[§2], Yuh Mochizuki[¶], Hisashi Hoshida[‖], Soichiro Kakuta[‡3], Chika Kondo-Kakuta[‡], Nobuo N. Noda[**], Fuyuhiko Inagaki[§], Takehiko Itoh[¶], Rinji Akada[‖], and Yoshinori Ohsumi[‡4]**

*From the [‡]Frontier Research Center, Tokyo Institute of Technology, Yokohama 226-8503, the [§]Department of Structural Biology, Faculty of Advanced Life Science, Hokkaido University, Sapporo 060-0812, the [¶]Laboratory of In Silico Functional Genomics, Graduate School of Bioscience and Biotechnology, Tokyo Institute of Technology, Yokohama 226-8501, the [‖]Department of Applied Molecular Bioscience, Yamaguchi University Graduate School of Medicine, Ube 755-8611, and the [**]Institute of Microbial Chemistry, Tokyo 141-0021, Japan*

**Background:** Autophagosome formation is mediated by multiple autophagy-related (Atg) proteins.
**Results:** Essential Atg proteins of *K. marxianus*, which have superior thermostability and solubility, are identified.
**Conclusion:** *K. marxianus* can be used as a novel organism to study autophagy.
**Significance:** *K. marxianus* proteins are broadly applicable as tools for *in vitro* studies, not only in autophagy field but also in other fields.

**Autophagy is a conserved degradation process in which autophagosomes are generated by cooperative actions of multiple autophagy-related (Atg) proteins. Previous studies using the model yeast *Saccharomyces cerevisiae* have provided various insights into the molecular basis of autophagy; however, because of the modest stability of several Atg proteins, structural and biochemical studies have been limited to a subset of Atg proteins, preventing us from understanding how multiple Atg proteins function cooperatively in autophagosome formation. With the goal of expanding the scope of autophagy research, we sought to identify a novel organism with stable Atg proteins that would be advantageous for *in vitro* analyses. Thus, we focused on a newly isolated thermotolerant yeast strain, *Kluyveromyces marxianus* DMKU3-1042, to utilize as a novel system elucidating autophagy. We developed experimental methods to monitor autophagy in *K. marxianus* cells, identified the complete set of *K. marxianus* Atg homologs, and confirmed that each Atg homolog is engaged in autophagosome formation. Biochemical and bioinformatic analyses revealed that recombinant *K. marxianus* Atg proteins have superior thermostability and solubility as compared with *S. cerevisiae* Atg proteins, probably due to the shorter primary sequences of KmAtg proteins. Furthermore, bioinformatic analyses showed that more than half of *K. marxianus* open reading frames are relatively short in length. These features make *K. marxianus* proteins broadly applicable as tools for structural and biochemical studies, not only in the autophagy field but also in other fields.**

Macroautophagy (hereafter referred to as autophagy), a fundamental cellular process conserved from yeast to mammals, mediates bulk degradation of cytoplasmic proteins and organelles in response to starvation (1–4). Autophagy has attracted considerable interest in the fields of biological and medical sciences because it plays important roles in a variety of cellular events, including metabolic adaptation, stress response, quality control, development, tumor suppression, and renovation of cellular components (5–7). Morphologically, autophagy involves *de novo* formation of a double-membrane structure, called an autophagosome, that sequesters cytoplasmic materials. After the sequestration, the autophagosome fuses with lytic compartments (vacuoles in yeast and plants and lysosomes in mammals), leading to degradation of its contents (3, 4).

Previous studies using the yeast *Saccharomyces cerevisiae* identified nearly 40 autophagy-related (Atg)[5] proteins involved in various types of autophagy (3, 4, 8). Among these, 18 Atg proteins (Atg1-Atg10, Atg12-Atg14, Atg16-Atg18, Atg29, and Atg31), defined as core Atg proteins (1), are crucial for the process of autophagosome formation. These Atg proteins are functionally and hierarchically classified into six subgroups as follows: the Atg1 complex (Atg1, Atg13, Atg17, Atg29, and Atg31); a vesicular membrane protein required for the early step of autophagosome formation (Atg9); the autophagy-specific PtdIns 3-kinase complex (Atg6 and Atg14; also includes

* This work was supported in part by Grant-in-aid for Scientific Research on Innovative Areas 26111508 (to H. Y.) and Grant-in-aid for Specially Promoted Research 23000015 (to Y. O.) from the Ministry of Education, Culture, Sports, Science and Technology of Japan. The authors declare that they have no conflicts of interest with the contents of this article.
[S] This article contains supplemental Figs. S1–S4 and Tables S1–S3.
[1] To whom correspondence may be addressed. Tel.: 81-45-924-5879; Fax: 81-45-924-5121; E-mail: yamamoto-hayashi@iri.titech.ac.jp.
[2] Present address: Dept. of Structural Biology, St. Jude Children's Research Hospital, Memphis, TN 38105.
[3] Present address: Biomedical Research Center, Juntendo University School of Medicine, Tokyo 113–8421, Japan.
[4] To whom correspondence may be addressed. Tel.: 81-45-924-5879; Fax: 81-45-924-5121; E-mail: yohsumi@iri.titech.ac.jp.

[5] The abbreviations used are: Atg, autophagy-related; ALP, alkaline phosphatase; PAS, preautophagosomal structure; DSF, differential scanning fluorimetry; PE, phosphatidylethanolamine.

Vps15 and Vps34); the phosphatidylinositol 3-phosphate effector complex (Atg2 and Atg18); and two ubiquitin-like conjugation systems (Atg3, Atg4, Atg5, Atg7, Atg8, Atg10, Atg12, and Atg16). Consequently, most of the key findings concerning the molecular basis of autophagosome formation have been obtained in the model yeast *S. cerevisiae*. In particular, the members of the two ubiquitin-like conjugation systems have been well characterized, because several lines of structure-based analyses (9–15) and *in vitro* reconstitution studies (16–18) have provided critical insights into their molecular functions. However, these structural and biochemical studies have been limited to a subset of the Atg proteins, because the rest of Atg proteins are difficult to prepare as recombinant proteins and cannot be purified efficiently from yeast cells. Therefore, the detailed functions of these Atg proteins remain to be elucidated.

One of the major problems in preparation of recombinant Atg proteins, most of which have been derived thus far from *S. cerevisiae* and mammals, is the modest stability of these proteins. We predicted that recombinant proteins derived from thermotolerant organisms would exhibit superior stability against high temperature and chemical reagents relative to their counterparts from *S. cerevisiae*. As an illustration of this principle, a heat-resistant *Taq*DNA polymerase derived from the thermophilic bacterium *Thermus aquaticus* is widely used in polymerase chain reaction techniques (19), and recently, Amlacher *et al.* (20)succeeded in reconstituting the structural modules of nuclear pore complexes using proteins from the thermophilic fungus *Chaetomium thermophilum*. Hence, we attempted to utilize the thermotolerant yeast strain *Kluyveromyces marxianus* DMKU3-1042, which can grow at temperatures above 49 °C (21), because its Atg homologs are predicted to be thermostable and useful for structural and biochemical studies. In this study, we first identified the complete set of core Atg proteins of *K. marxianus* and then investigated their thermostability and solubility by biochemical analyses. Complementation assays showed that the *K. marxianus* Atg homologs can functionally replace their counterparts in *S. cerevisiae* cells. We propose that *K. marxianus* could be useful as a new model organism for further elucidation of the molecular details of autophagy.

## Experimental Procedures

*Yeast Strains, Media, Plasmids, and Other Materials*—Yeast strains used in this study are listed in supplemental Table 1. For cultivation of *S. cerevisiae* and *K. marxianus* cells, standard protocols of *S. cerevisiae* studies were used (22). Yeast cells were cultured at 30 °C in nutrient-rich medium YPD (1% yeast extract, 2% bacto-peptone, 2% glucose) or SD/CA (0.17% yeast nitrogen base without amino acids and ammonium sulfate, 0.5% ammonium sulfate, 0.5% casamino acids, 2% glucose) supplemented with 20 μg/ml adenine, 20 μg/ml uracil, and/or 20 μg/ml tryptophan. To induce autophagy, yeast cells were transferred to nitrogen starvation medium SD(−N) (0.17% yeast nitrogen base without amino acids and ammonium sulfate, 2% glucose) or treated with 0.2 μg/ml rapamycin (Sigma). Gene deletions of *S. cerevisiae* cells were performed by using pFA6a-kanMX6, pFA6a-hphNT1, and pFA6a-natNT2 plasmids as reported previously (23). Gene deletions of *K. marxianus* cells were performed by using pFA6a-kanMX6, pFA6a-hphNT1, and pFA6a-natNT2 plasmids as reported previously (24). The *K. marxianus* cells expressing GFP-KmAtg8 were constructed; a DNA fragment, including the Km*ATG8* promoter, the Km*ATG8* gene, and the Km*ATG8* terminator (from 1000-bp upstream region of the initiation codon to 250-bp downstream region of the termination codon of the Km*ATG8* gene), was amplified from genomic DNA of *K. marxianus* and cloned into pFA6a-kanMX6 (23). A BamHI site was introduced into the resultant plasmid just downstream of the first codon of the Km*ATG8* gene by QuikChange site-directed mutagenesis (Stratagene), and a DNA fragment encoding GFP was inserted into the BamHI site, yielding pFA6a-GFP-KmAtg8-kanMX6. A DNA fragment, including the Km*ATG8* promoter, the *GFP* gene, the Km*ATG8* gene, and the Km*ATG8* terminator, was amplified from pFA6a-GFP-KmAtg8-kanMX6 and integrated into the *K. marxianus* chromosome as reported previously (24). The plasmids for integration of GFP-KmAtg8$^{FG}$ and GFP-KmAtg8$^{FA}$ were constructed by QuikChange site-directed mutagenesis (Stratagene). The plasmids for expression of KmAtg proteins in *S. cerevisiae* cells under control of their own promoter were constructed as follows: a DNA fragment, including the Km*ATG* promoter, the Km*ATG* gene, and the Km*ATG* terminator (from 1000-bp upstream region of the initiation codon to 250-bp downstream region of the termination codon of the Km*ATG* gene), was amplified from genomic DNA of *K. marxianus* and cloned into pRS316 (25) by using an In-Fusion cloning kit (Clontech). The plasmids for expression of KmAtg proteins in *S. cerevisiae* cells under control of Sc*TDH3* (GPD) promoter were constructed as follows: a DNA fragment including the Km*ATG* gene was amplified from genomic DNA of *K. marxianus* and cloned into pRS316-GPDpro-PGKterm by using an In-Fusion cloning kit (Clontech).

*Electron Microscopy*—Cells were sandwiched between copper grids and rapidly frozen in liquid propane (−175 °C) using Leica EM CPC (Leica), followed by substitution fixation in 2% osmium tetroxide dissolved in acetone containing 3% distilled water. Specimens were embedded in Quetol-651, sectioned, and observed with a transmission electron microscope (H-7500, Hitachi).

*Fluorescence Microscopy*—Fluorescence microscopy was performed at room temperature, as reported previously (26), by using an inverted fluorescence microscope (IX-71, Olympus) equipped with an electron-multiplying CCD camera (ImagEM, C9100-13, Hamamatsu Photonics) and 150× TIRF objective (UAPON 150XOTIRF, NA/1.45, Olympus). A 488-nm blue laser (20 milliwatts, Spectra-Physics) and a 561-nm yellow laser (25 milliwatt, Cobalt) were used for excitation of GFP and FM4-64, respectively. To increase image intensity and decrease background intensity, specimens were illuminated with a highly inclined laser beam (27). For simultaneous observation of GFP and FM4-64, both lasers were combined and guided without an excitation filter, and the fluorescence was filtered with a Di01-R488/561-25 dichroic mirror (Semrock) and an Em01-R488/568-25 bandpass filter (Semrock) and separated into two channels using a U-SIP splitter (Olympus) equipped with a DM565HQ dichroic mirror (Olympus). The fluorescence was

further filtered with an FF02-525/50-25 bandpass filter (Semrock) for the GFP channel and an FF01-624/40-25 bandpass filter (Semrock) for the FM4-64 channel. Images were acquired using AQUACOSMOS software (Hamamatsu Photonics) and processed using MetaMorph software (Molecular Devices).

*Preparation of Recombinant Proteins*—ScAtg3, ScAtg7, and ScAtg8 were prepared as described previously (17). ScAtg10 was prepared as described previously (28). KmAtg7 and KmAtg10 were prepared as described previously (29). KmAtg3 and KmAtg8 were prepared as described previously (30). For NMR spectrometry of ScAtg10 and KmAtg10, $^{15}$N-labeled proteins were prepared by growing *Escherichia coli* cells in M9 medium using $^{15}NH_4Cl$ as the sole nitrogen source.

*Differential Scanning Fluorimetry*—Recombinant proteins (20 $\mu$M) in 50 mM Tris-HCl, pH 7.5, 150 mM NaCl, 1 mM DTT supplemented with 50,000th volume of SYPRO Orange (Invitrogen) were heated from 25 to 95 °C with a heating rate of 1 °C/min. The fluorescence intensities were measured using an Mx3005P Real Time quantitative PCR system (Agilent Technologies) with excitation at 490 nm and emission at 530 nm. The midpoint temperature of the unfolding transition ($T_m$) was determined using GraphPad Prism software (GraphPad Software) from curve fitting to a Boltzmann equation (31).

*NMR Spectrometry*—NMR experiments were carried out at 298 K on a Varian UNITY INOVA 600 spectrometer. The sample solution of the $^{15}$N-labeled ScAtg10 in 20 mM Tris-HCl, pH 7.5, 10 mM DTT, and the $^{15}$N-labeled KmAtg10 in 20 mM phosphate buffer, pH 6.8, 100 mM NaCl were prepared for measurements of $^{1}$H-$^{15}$N HSQC spectra. The NMR spectra were processed by NMRpipe (32), and data analysis was conducted using the Sparky program (33).

## Results

*Bioinformatic Analyses of the Comprehensive Genome Sequence of the Novel Thermotolerant Yeast Strain K. marxianus DMKU3-1042*—One prospective approach to further understanding autophagy is utilization of novel organisms with advantageous features for investigating the molecular functions of Atg proteins. Here, we focused on a newly isolated thermotolerant yeast strain, *K. marxianus* (Km) DMKU3-1042, which can grow at temperatures up to 49 °C (21) and whose genome sequence was determined recently (34). By bioinformatic approaches, we compared all of the open reading frames (ORFs) of the thermotolerant yeast *K. marxianus* and the model yeast *S. cerevisiae*. At first, we analyzed overall sequence alignments between *K. marxianus* and *S. cerevisiae* proteins (3,355 ORF pairs from 4,564 *K. marxianus* ORFs and 5,882 *S. cerevisiae* ORFs) using the BLAST and ClustalW web servers (Fig. 1*A*). These analyses showed that housekeeping proteins such as ribosomal proteins, mitochondrial proteins, and proteins involved in metabolism and nutrient utilization are nearly of the same length in *S. cerevisiae* and *K. marxianus* (Fig. 1*A* and supplemental Table 2), potentially due to the fundamental importance of these proteins in cell proliferation. By contrast, several subgroups of *K. marxianus* proteins, annotated as involved in protein degradation, chromosome segregation, and morphogenesis, had significantly shortened primary sequences (Fig. 1*A* and supplemental Table 2), potentially reflecting genetic diversity caused by adaptation to high temperature conditions, implying that these shortened *K. marxianus* proteins could have higher thermostability as compared with the *S. cerevisiae* counterparts.

Bioinformatic analyses also showed that almost half of the *K. marxianus* proteins (48.7%, 1,635 ORFs) are shorter than their *S. cerevisiae* counterparts (Fig. 1*B* and supplemental Table 2), and the rest are nearly the same length (24.7%, 828 ORFs) or longer (26.6%, 892 ORFs). The total numbers of the comparable amino acid residues were 1,777,544 from *K. marxianus* ORFs and 1,799,483 from *S. cerevisiae* ORFs (supplemental Table 2), indicating that *K. marxianus* proteins are on average 1.22% shorter than *S. cerevisiae* proteins.

Next, we analyzed the predicted unfoldability of *K. marxianus* and *S. cerevisiae* proteins using the FoldIndex web server (35). FoldIndex scores calculated from the amino acid sequences of *K. marxianus* and *S. cerevisiae* (3,355 ORF pairs) revealed that *K. marxianus* proteins are relatively less disordered than their *S. cerevisiae* counterparts (Fig. 1*C* and supplemental Table 3); the average scores of *K. marxianus* and *S. cerevisiae* ORFs were 0.0969 and 0.0934, respectively (Fig. 1*C*, $p = 7.14E-8$). In particular, the *K. marxianus* proteins that are shorter than *S. cerevisiae* counterparts are significantly less disordered (Fig. 1*D*, *left*, $p = 5.08E-14$). Additionally, *K. marxianus* proteins that are nearly the same length as their *S. cerevisiae* counterparts are also relatively less disordered (Fig. 1*D*, *middle*, $p = 1.26E-6$). Taken together, we found that almost half of the *K. marxianus* proteins are shorter in length and have a more ordered secondary structure than their *S. cerevisiae* counterparts, which might contribute to the superior thermotolerance of *K. marxianus*.

*Identification of Atg Homologs in K. marxianus*—Homology searches of the *K. marxianus* genome sequence identified a complete set of core KmAtg proteins by their sequence similarity to those of *S. cerevisiae* (Sc). As shown in Fig. 1*B*, most KmAtg proteins are apparently shorter than ScAtg proteins (located on the *left side* of the *blue box* indicating Km < *Sc* in Fig. 1*B*) and have relatively low identity (Figs. 1*B* and 2*A*), as compared with other housekeeping *K. marxianus* proteins (Fig. 1*A*). These features of KmAtg proteins strongly raised the possibility that KmAtg proteins has superior thermostability as compared with the ScAtg counterparts. In addition to KmAtg proteins, we identified several vacuolar enzymes frequently used in the autophagy field (Pep4, Prb1, Pho8, and Ape1) (Fig. 2*A*). Therefore, we first tried to develop experimental methods to assess autophagy in *K. marxianus* cells.

*Probes for Monitoring Autophagy in K. marxianus Cells*—One of the easiest ways to evaluate the progression of autophagy is to monitor intravacuolar accumulation of autophagy-related structures called autophagic bodies (36). Thus, we performed several morphological analyses, including electron microscopy and fluorescence microscopy, to examine autophagy in *K. marxianus* cells. To observe accumulation of autophagic bodies, we deleted the Km*PEP4* gene from *K. marxianus* cells; ScPep4 is a putative master enzyme required for activation of the vacuolar hydrolases responsible for degradation of autophagic bodies (36), and KmPep4 is highly conserved in *K. marxianus* as a single gene product (Fig. 2*A*, *73.8% iden-*

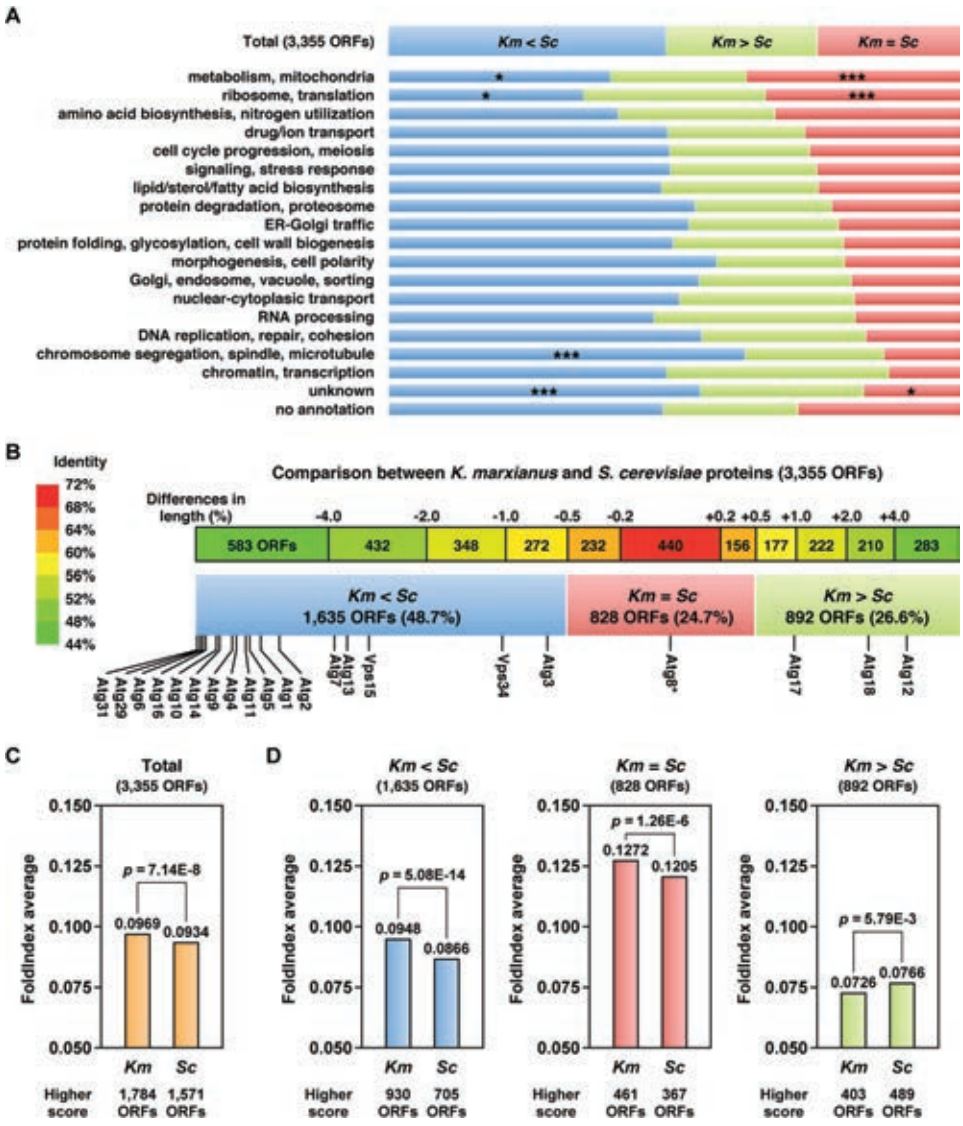


FIGURE 1. **Bioinformatic analyses of the comprehensive genome sequences of *K. marxianus* and *S. cerevisiae*.** *A,* comparable ORFs aligned using the BLAST server were classified into three subgroups according to their relative lengths (see also supplemental Table 2). The comparable ORFs (total 3,355 ORF pairs) were annotated according to their functions. *Asterisks*, significantly fewer than in total ORFs ($p < 0.005$); *triple asterisks*, significantly more than in total ORFs ($p < 0.005$). *B,* almost half of all *K. marxianus* proteins are shorter than their *S. cerevisiae* counterparts. *Km < Sc*, the *K. marxianus* proteins are >0.5% shorter than the *S. cerevisiae* counterparts (1,635 ORFs in *blue*); *Km = Sc*, the *K. marxianus* proteins are nearly the same length as the *S. cerevisiae* counterparts (828 ORFs in *red*); *Km > Sc*, the *K. marxianus* proteins are >0.5% longer than the *S. cerevisiae* counterparts (892 ORFs in *green*). Identities of the comparable ORFs (3,355 ORF pairs) from *A* were calculated using the LALIGN server. *Asterisk,* mature form of Atg8. *C,* unfoldability scores of all comparable *K. marxianus* and *S. cerevisiae* ORFs (3,355 ORF pairs) were assessed using the FoldIndex server (see also supplemental Table 3). Mean FoldIndex scores were analyzed statistically. *D,* mean FoldIndex scores of three subgroups in *B* were analyzed as in *C*.

*tical to ScPep4*). Electron microscopy revealed that in Km*pep4*Δ cells treated with the autophagy-inducing drug rapamycin, a large number of autophagic bodies accumulated in the vacuolar lumen (Fig. 2*B*, *middle panel*). This observation indicates that upon rapamycin treatment, autophagy was efficiently induced in *K. marxianus* cells. Next, we deleted the Km*ATG8* gene to determine whether KmAtg8 contributes to autophagosome formation, because Atg8 and its mammalian homolog LC3 have been widely used as an autophagosomal marker (37, 38); furthermore, among the KmAtg homologs, KmAtg8 has the highest identity to its *S. cerevisiae* counterpart (Fig. 2*A*, *85.3% identical to ScAtg8*). As expected, electron microscopy revealed that no autophagic bodies formed in the absence of KmAtg8 (Fig. 2*B*, *right panel*), confirming that KmAtg8 is involved in autophagosome formation in *K. marxianus*. We next developed an alkaline phosphatase (ALP) assay, a method for quantitatively assessing autophagic activity that was originally established in *S. cerevisiae* (39). The vacuolar alkaline phosphatase KmPho8 is also conserved as a single gene product in *K. marxianus* (Fig. 2*A*, *58.1% identical to ScPho8*). A truncated form of KmPho8 that lacks its signal sequence, KmPho8ΔN44, is expressed in the cytoplasm, and its transport into the vacuole as an autophagosomal content and subsequent activation by vacuolar hydrolases can be quantitatively measured. In wild-type cells, ALP activity increased significantly upon nutrient starvation (Fig. 2*C*), and this increase was strictly dependent on the presence of the ALP probe KmPho8ΔN44 and the vacuolar hydrolases KmPep4 and KmPrb1 (Fig. 2*C*, *left panel*). By using

A

| | Atg1 | Atg2 | Atg3 | Atg4 | Atg5 | Atg6 | Atg7 | Atg8* | Atg9 | Atg10 | Atg11 | Atg12 | Atg13 |
|---|---|---|---|---|---|---|---|---|---|---|---|---|---|
| *S. cerevisiae* | 897 aa | 1592 aa | 310 aa | 494 aa | 294 aa | 557 aa | 630 aa | 116 aa | 997 aa | 167 aa | 1178 aa | 186 aa | 738 aa |
| *K. marxianus* | 836 aa | 1499 aa | 308 aa | 451 aa | 271 aa | 466 aa | 606 aa | 116 aa | 906 aa | 147 aa | 1084 aa | 195 aa | 712 aa |
| Differences in length | -6.80% | -5.84% | -0.65% | -8.70% | -7.82% | -16.3% | -3.81% | 0% | -9.13% | -12.0% | -7.98% | +4.84% | -3.52% |
| Identity | 52.4% | 30.8% | 56.5% | 45.3% | 31.4% | 40.8% | 49.5% | 85.3% | 49.0% | 33.7% | 28.9% | 36.5% | 37.1% |

| | Atg14 | Atg16 | Atg17 | Atg18 | Atg29 | Atg31 | Vps15 | Vps34 | Pep4 | Prb1 | Pho8 | Ape1 |
|---|---|---|---|---|---|---|---|---|---|---|---|---|
| *S. cerevisiae* | 344 aa | 150 aa | 417 aa | 500 aa | 213 aa | 196 aa | 1454 aa | 875 aa | 405 aa | 635 aa | 566 aa | 514 aa |
| *K. marxianus* | 305 aa | 126 aa | 421 aa | 513 aa | 162 aa | 139 aa | 1412 aa | 866 aa | 408 aa | 553 aa | 546 aa | 524 aa |
| Differences in length | -11.3% | -16.0% | +0.96% | +2.60% | -23.4% | -29.1% | -2.89% | -1.03% | +0.74% | -12.9% | -3.53% | +1.95% |
| Identity | 27.1% | 45.6% | 33.1% | 59.9% | 48.2% | 34.4% | 42.8% | 60.5% | 73.8% | 66.7% | 58.1% | 60.8% |

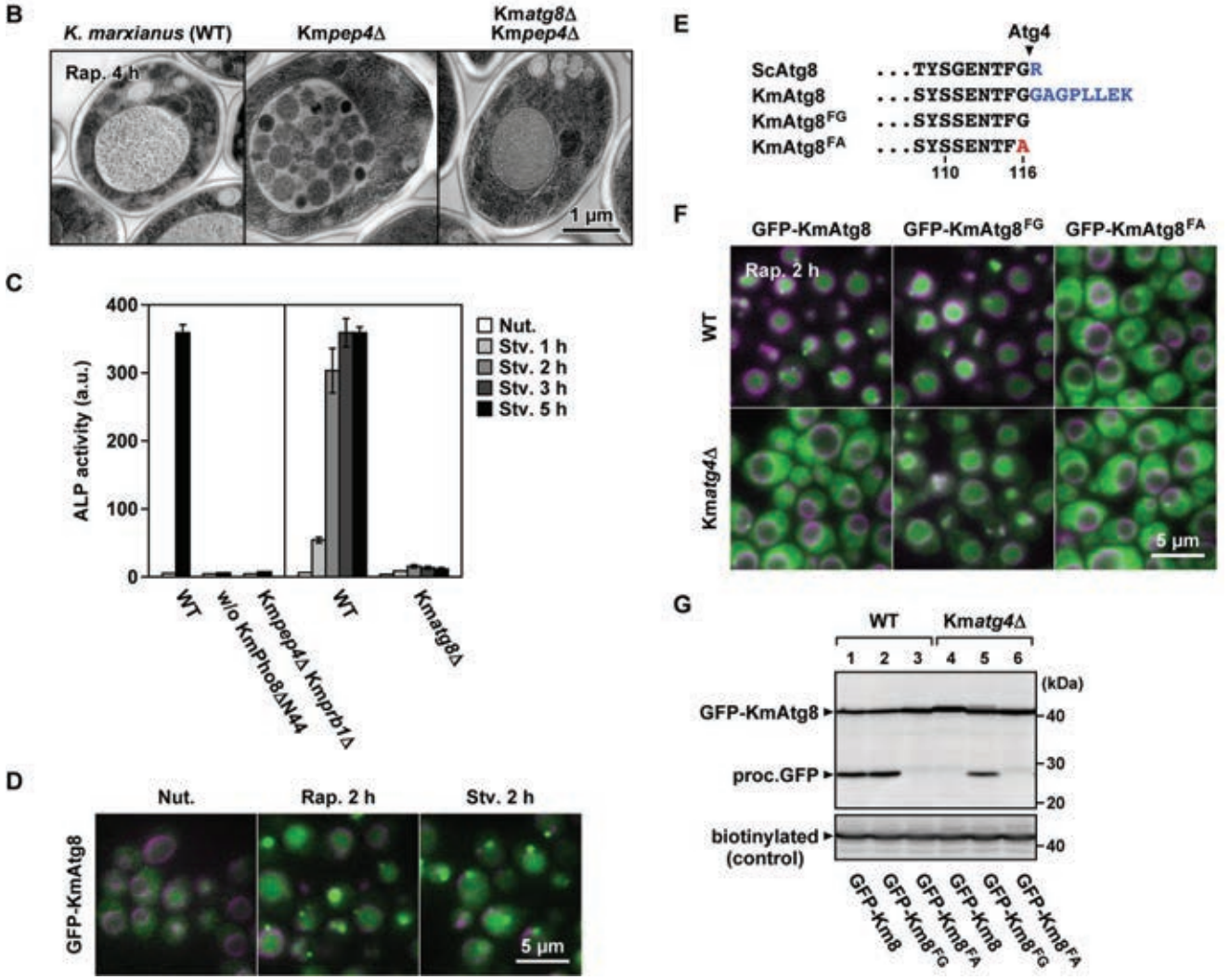


FIGURE 2. **Identification of Atg homologs and probes for monitoring autophagy in *K. marxianus*.** *A,* Atg homologs in *K. marxianus*. Most KmAtg proteins are shorter than their ScAtg counterparts (*red*). *Asterisk,* mature form of Atg8. *B,* KmAtg8 is required for autophagosome formation in *K. marxianus*. *K. marxianus* wild-type (*WT*), Km*pep4*Δ, and Km*pep4*Δ Km*atg8*Δ cells were grown at 30 °C, treated with rapamycin for 4 h, and subjected to electron microscopy. *C,* KmAtg8 is essential for *K. marxianus* autophagy. *K. marxianus* wild-type (*WT*), Km*pep4*Δ Km*prb1*Δ, and Km*atg8*Δ cells expressing an N-terminally truncated variant of KmPho8 (*KmPho8ΔN44*) were grown at 30 °C and then shifted to nitrogen-starvation medium. Km*pho8*Δ cells were used as a control not expressing the probe KmPho8ΔN44 (without KmPho8ΔN44). After starvation for 5 h, the cells were harvested, and ALP activities were measured. *a.u.*, arbitrary unit. *D,* GFP-KmAtg8 is transported into the vacuole. Wild-type *K. marxianus* cells expressing GFP-KmAtg8 (*green*) were treated with FM4-64 (*magenta*). The cells were grown at 30 °C (*Nut.*) and then treated with rapamycin for 2 h (*Rap. 2 h*) or incubated in nitrogen-starvation medium for 2 h (*Stv. 2 h)*. The cells were observed by fluorescence microscopy. *E,* C-terminal regions of ScAtg8 and KmAtg8. Atg8 is synthesized as a precursor form with an additional segment at its C terminus (*blue*) and cleaved by Atg4 to be converted into the mature form. KmAtg8$^{FG}$ is a truncated variant that mimics a mature form. KmAtg8$^{FA}$ contains an Ala substitution at residue 116 (*red*). *F,* KmAtg4 is responsible for the maturation of KmAtg8. GFP-KmAtg8, GFP-KmAtg8$^{FG}$, and GFP-KmAtg8$^{FA}$ (*green*) were expressed in *K. marxianus* wild-type and Km*atg4*Δ cells. The cells were treated with FM4-64 (*magenta*), treated with rapamycin for 2 h, and then observed by fluorescence microscopy. *G,* GFP-processing assay in *K. marxianus*. The *K. marxianus* cells used in *F* were treated with rapamycin for 1 h, and then total lysates were prepared. Samples were subjected to immunoblot analysis using anti-GFP antibody and streptavidin-HRP as a loading control (biotinylated). *proc.GFP* indicates a processed form of the GFP moiety.

this assay, we measured autophagic activity in Km*atg8*Δ cells. In the absence of KmAtg8, no autophagic activity was detected (Fig. 2*C*, *right panel*), suggesting that KmAtg8 is essential for *K. marxianus* autophagy. From these results, we concluded that the ALP assay is applicable for *K. marxianus* studies.

Atg8 (LC3 in mammals) is known to be localized on autophagosomal membranes (37, 38). Hence, we constructed *K. marxianus* cells expressing GFP-KmAtg8 under the control of the Km*ATG8*'s own promoter. Fluorescence microscopy revealed that after rapamycin treatment (Fig. 2*D*, *middle panel*) or nutrient starvation (Fig. 2*D*, *right panel*), a significant portion of GFP-KmAtg8 was transported into the vacuole. These observations clearly indicate that GFP-KmAtg8 can be used as a probe to assess the progression of autophagy in *K. marxianus* cells.

In *S. cerevisiae* cells, the ubiquitin-like protein ScAtg8 is synthesized as a precursor form with an additional Arg residue at its C terminus; the Arg residue is subsequently cleaved by the cysteine protease ScAtg4 (40, 41), resulting in conversion of ScAtg8 into a 116-residue mature form in which the C-terminal Gly residue is exposed (Fig. 2*E*). KmAtg8 is also predicted to be synthesized as a precursor form with an additional 8-residue sequence, which is cleaved by KmAtg4 to generate the 116-residue mature form (Fig. 2*E*). To confirm the involvement of KmAtg4 in the cleavage of KmAtg8, we constructed a truncated form of KmAtg8 in which the C-terminal Gly residue (KmAtg8$^{FG}$) is exposed, which is predicted to be functional as the mature form (Fig. 2*E*). In the absence of KmAtg4, wild-type GFP-KmAtg8 was not transported into the vacuolar lumen but instead dispersed in the cytoplasm (Fig. 2*F*, *lower left panel*). By contrast, GFP-KmAtg8$^{FG}$ was transported to some extent into the vacuolar lumen even in the absence of KmAtg4 (Fig. 2*F*, *lower middle panel*), suggesting that KmAtg8$^{FG}$ bypassed the requirement for cleavage by KmAtg4. We also confirmed that the GFP-KmAtg8$^{FA}$ mutant (Fig. 2*E*), which contains an Ala substitution at residue 116, preventing its conjugation with a lipid phosphatidylethanolamine (PE) (16), was not transported into the vacuolar lumen even in wild-type cells (Fig. 2*F*, *right upper panels*). From these results, we conclude that KmAtg4 is responsible for the maturation of KmAtg8.

We next examined the levels of GFP-KmAtg8 in the vacuole by immunoblot analysis. In wild-type cells, GFP-KmAtg8 was efficiently transported into the vacuole and processed to yield an ~28-kDa GFP fragment (Fig. 2*G*, *lane 1*), because the GFP moiety is resistant to vacuolar proteases (42). By contrast, no GFP fragment was detected in Km*atg4*Δ cells (Fig. 2*G*, *lane 4*), indicating that GFP-KmAtg8 was not transported into the vacuole in the absence of KmAtg4. In addition, GFP-KmAtg8$^{FG}$ yielded the GFP fragment efficiently in wild-type cells and at somewhat lower levels in Km*atg4*Δ cells (Fig. 2*G*, *lanes 2* and *5*), whereas GFP-KmAtg8$^{FA}$ yielded no GFP fragment even in wild-type cells (Fig. 2*G*, *lanes 3* and *6*). These results suggest that KmAtg8 and KmAtg4 function in a similar manner to their *S. cerevisiae* counterparts. Furthermore, the levels of the processed GFP fragment detected in the immunoblot analysis (Fig. 2*G*) were well correlated with the levels of intra-vacuolar GFP-KmAtg8 observed by fluorescence microscopy (Fig. 2*F*). These observations indicate that GFP-KmAtg8 can be used as a probe to monitor *K. marxianus* autophagy in both fluorescence microscopy and immunoblot analysis.

*KmAtg Proteins Are Involved in Autophagosome Formation in K. marxianus Cells*—Using GFP-KmAtg8 as a probe, we examined the involvement of other KmAtg proteins in autophagy. For this purpose, we constructed GFP-KmAtg8 strains lacking each Km*ATG* gene. Fluorescence microscopy revealed that in the absence of core KmAtg homologs, the vacuolar transports of GFP-KmAtg8 were not observed at all (Fig. 3*A*), indicating that these KmAtg proteins are certainly involved in autophagy in *K. marxianus*. Their phenotypes could be classified into two groups. In cells depleted of KmAtg1, KmAtg2, KmAtg6, KmAtg9, KmAtg13, KmAtg14, or KmAtg18, GFP-KmAtg8 formed a punctate structure in proximity to the vacuolar membrane, which appeared to be the preautophagosomal structure (PAS) observed in *S. cerevisiae* cells (43). In contrast, the bright PAS puncta were barely detectable in cells depleted of KmAtg3, KmAtg4, KmAtg5, KmAtg7, KmAtg10, KmAtg12, or KmAtg16, all of which are members of the two ubiquitin-like conjugation systems (Fig. 3, *A* and *B*, *green bars*). These observations were consistent with those in *S. cerevisiae*, in which PAS assembly of GFP-ScAtg8 strictly requires the ubiquitin-like conjugation systems (44). We also observed that in addition to the bright PAS puncta, small GFP-KmAtg8-positive dots were observed in *K. marxianus* cells defective of the two ubiquitin-like conjugation systems (Fig. 3*B*, *gray bars*), which may imply additional functions of KmAtg8.

Fluorescence microscopy also revealed that KmAtg11, KmAtg17, KmAtg29, and KmAtg31 were not essential for the vacuolar transport of GFP-KmAtg8 (Fig. 3*C*, *upper panels*). Immunoblot analysis also showed that the GFP fragment derived from GFP-KmAtg8 was detected (although at somewhat reduced levels) in the absence of KmAtg11, KmAtg17, KmAtg29, or KmAtg31 (Fig. 3*D*, *lanes 10–13*), indicating that GFP-KmAtg8 was at least partially transported into the vacuole in these cells. Previous studies using *S. cerevisiae* have shown that ScAtg17, ScAtg29, and ScAtg31 form a ternary complex that organizes the PAS scaffold responsible for starvation-induced autophagy (45) and that ScAtg11 plays a similar role to the ScAtg17-ScAtg29-ScAtg31 complex under nutrient-rich conditions (42). Therefore, we constructed the double-deletion mutants Km*atg11*Δ Km*atg17*Δ, Km*atg11*Δ Km*atg29*Δ, and Km*atg11*Δ Km*atg31*Δ. In all of the double mutants, GFP-KmAtg8 was not transported into the vacuole but was largely dispersed in the cytoplasm (Fig. 3*C*, *lower panels*). These results suggest that KmAtg11 has a redundant function with KmAtg17, KmAtg29, and KmAtg31 in *K. marxianus* cells. Previous *S. cerevisiae* studies showed that ScAtg11 is involved in the biosynthesis of the vacuolar aminopeptidase Ape1 under nutrient-rich conditions (46, 47). Ape1 is synthesized in the cytoplasm as a precursor form (prApe1) and subsequently transported into the vacuole via selective autophagy, called the cytoplasm-to-vacuole targeting pathway, to be processed into the mature form (mApe1). In *K. marxianus* cells, prKmApe1 was barely converted to the mature form in the absence of KmAtg11 under nutrient-rich conditions (Fig. 3*D*, *lane 2*), suggesting that KmAtg11 functions in the cytoplasm-to-vacuole targeting pathway in *K. marxianus* cells. Intriguingly, as judged

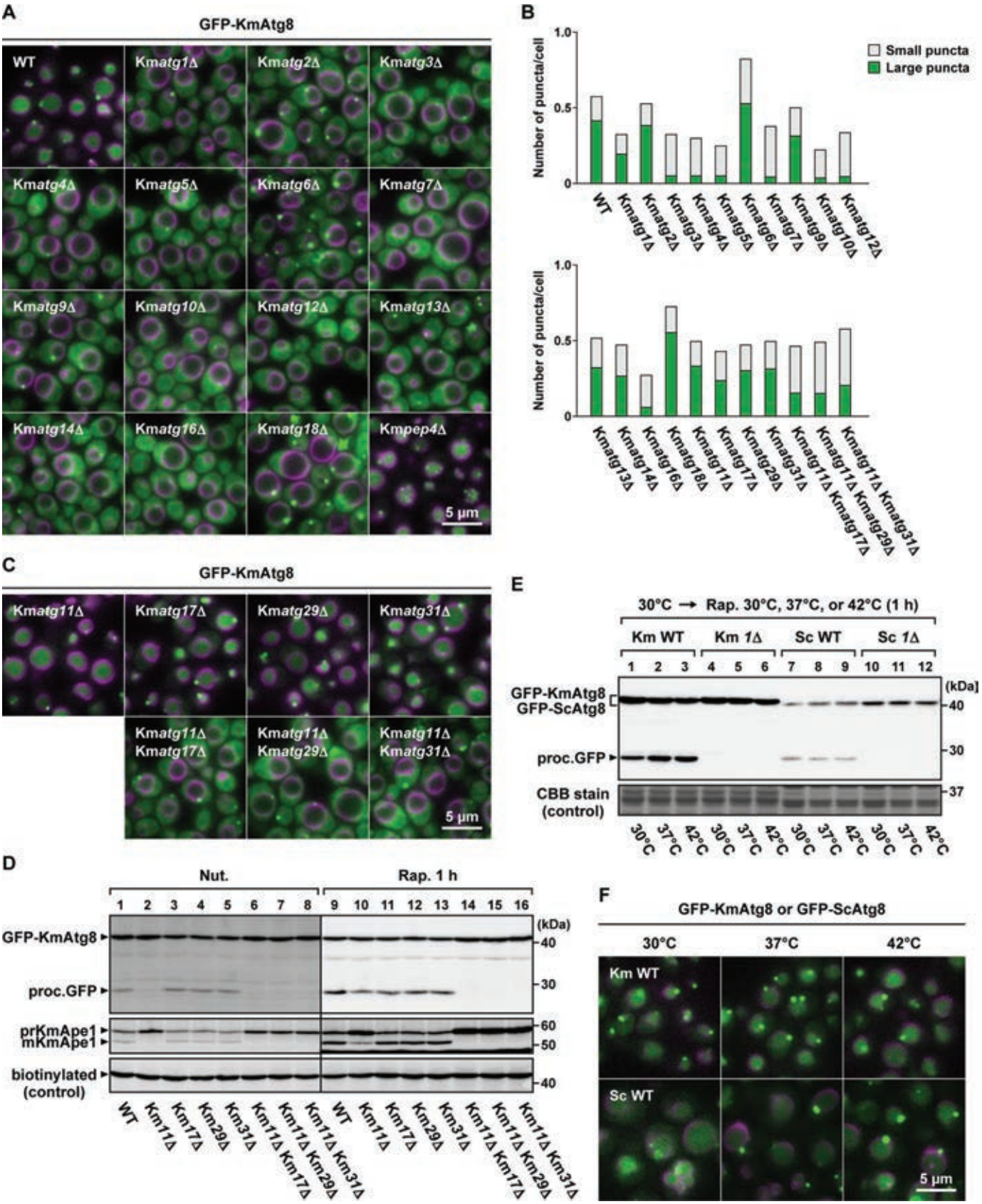

by a reduction in the level of the processed GFP fragment (Fig. 3*D*, *lane 10*), KmAtg11 is required not only for selective autophagy under nutrient-rich conditions but also for starvation-induced bulk autophagy (Fig. 3*D*, *lane 10*) to nearly the same extent as KmAtg17, KmAtg29, and KmAtg31 (Fig. 3*D*, *lanes 11–13*). These results suggest that although ScAtg11 is specifically involved in selective autophagy in *S. cerevisiae*, KmAtg11 plays an important role in bulk autophagy even under starvation conditions in *K. marxianus*. Taken together, these data indicate that as well as the core KmAtg proteins, KmAtg11, KmAtg17, KmAtg29, and KmAtg31 are also involved in bulk autophagy in *K. marxianus*.

*Autophagic Activity Is Enhanced under High Temperature Conditions in K. marxianus but Reduced in S. cerevisiae*—We next investigated whether high temperature stress induces autophagy in *K. marxianus* and *S. cerevisiae* cells. Under nutrient-rich conditions, neither the cytoplasm-to-vacuole targeting pathway nor autophagy was induced by heat stress at 37 or 42 °C in both *K. marxianus* and *S. cerevisiae* cells.[6] By combination of rapamycin treatment and heat stress, GFP-KmAtg8 efficiently yielded GFP fragments (Fig. 3*E*, *lanes 2* and *3*), indicating that autophagic activity is enhanced by heat stress in *K. marxianus*. By contrast, the vacuolar transport of GFP-ScAtg8 was reduced by heat stress in *S. cerevisiae* (Fig. 3*E*, *lanes 8* and *9*), and GFP-ScAtg8 highly accumulated at the perivacuolar sites under high temperature conditions (Fig. 3*F*). These observations suggest that ScAtg proteins were somewhat inactivated by heat stress, which also represents clear advance of *K. marxianus* in elucidation of mechanisms of autophagy induction against the high temperature stress.

*KmAtg Proteins Complement the Functions of ScAtg Proteins in S. cerevisiae*—We next investigated to what extent KmAtg proteins suppress autophagic defects caused by the depletion of ScAtg proteins in *S. cerevisiae*. To this end, we examined the maturation of prApe1 in rapamycin-treated cells, allowing highly sensitive assessment of autophagosome formation. In the absence of core ScAtg proteins, prApe1 was not transported into the vacuole and therefore not converted to mApe1 (Fig. 4*A*, except for Sc*atg13*Δ cells because of their partial phenotype). Upon exogenous expression of KmAtg proteins under the control of their own promoters (~1,000-bp upstream region of each Km*ATG* gene), prApe1 was modestly converted to mApe1 in most cases (Fig. 4*A*, *lanes 3, 5, 7, 9, 11, 13, 15, 18, 20,* and *24*), suggesting that these KmAtg proteins can at least partly complement deletion mutants of their ScAtg counterparts. In the cases of KmAtg5, KmAtg7, KmAtg10, KmAtg12, and KmAtg16, mApe1 was not detected at all (Fig. 4*A*, *lanes 22, 26, 28, 30,* and *32*), probably due to insufficient expression from the Km*ATG* promoters in *S. cerevisiae* cells. Therefore, we expressed these KmAtg proteins under control of the GPD promoter (Fig. 4*B*). Under these expression conditions, KmAtg7, KmAtg10, and KmAtg12 suppressed defects in maturation of prApe1 (Fig. 4*B*, *lanes 7, 10,* and *13*), suggesting that these proteins were functional in *S. cerevisiae*. By contrast, as judged by the maturation of prApe1, KmAtg5 and KmAtg16 failed to complement the functions of their *S. cerevisiae* counterparts. However, Sc*atg5*Δ cells expressing KmAtg5 yielded an extra band detected by anti-ScAtg12 antibodies (Fig. 4*B*, *lane 4*). This extra band migrated faster than that of the ScAtg12-ScAtg5 conjugate, one of the key products of the ubiquitin-like conjugation reaction (48). Based on the molecular weights of ScAtg5 (294 residues, 33.6 kDa) and KmAtg5 (271 residues, 31.2 kDa), it is conceivable that this extra band corresponds to the ScAtg12-KmAtg5 conjugate, the putative product of heterogeneous conjugation. Because ScAtg5 interacts directly with ScAtg16 in *S. cerevisiae*, we predicted that the ScAtg12-KmAtg5 conjugate would become functional in the presence of cognate KmAtg16 (49, 50). As expected, co-expression of KmAtg5 and KmAtg16 led to efficient conversion of prApe1 into mApe1 (Fig. 4*C*, *lanes 4* and *8*), indicating that the proper interaction between KmAtg5 and KmAtg16 is required for their functions. Based on the results of these complementation assays, which demonstrated the functions of KmAtg proteins, we conclude that the fundamental molecular mechanisms underlying autophagosome formation are conserved between *S. cerevisiae* and *K. marxianus*.

*KmAtg Proteins Are Thermostable Relative to ScAtg Proteins*—As compared with the ScAtg proteins, most of the KmAtg proteins are relatively short in length (Fig. 2*A*); sequence alignments between ScAtg and KmAtg proteins revealed that most ScAtg proteins contain several insertions (supplemental Figs. S1–S4). Thus, we assessed the thermostability of the KmAtg proteins. To date, four recombinant Atg proteins derived from both *S. cerevisiae* and *K. marxianus* cells (Atg3, Atg7, Atg8, and Atg10) have been prepared efficiently. Hence, we assessed the thermostability of these recombinant proteins by differential scanning fluorimetry (DSF). As compared with the ScAtg homologs, KmAtg3, KmAtg7, and KmAtg10 had relatively high $T_m$ values (*i.e.* the midpoint temperature at which they unfold). These data indicate that KmAtg3, KmAtg7, and KmAtg10 have superior thermostability relative to their *S. cerevisiae* counterparts (Fig. 5*A*).

We also analyzed their thermostability using an *in vitro* ubiquitin-like conjugation assay, a well established reconstitution system consisting of Atg7 (E1 enzyme), Atg3 (E2 enzyme), Atg8 (ubiquitin-like protein), and PE-containing liposomes (16).

[6] H. Yamamoto and Y. Ohsumi, unpublished data.

FIGURE 3. **Core KmAtg proteins are involved in autophagosome formation in *K. marxianus*.** *A* and *B,* GFP-KmAtg8 (*green*) was expressed in *K. marxianus* cells lacking each Km*ATG* gene. The cells were treated with FM4-64 (*magenta*), treated with rapamycin for 2 h, and then observed by fluorescence microscopy. *C,* numbers of GFP-KmAtg8 puncta per cell in *A* and *B*. Numbers of large puncta (fluorescence intensity, >30,000) and small puncta (fluorescence intensity, <30,000) are indicated by *green* and *gray bars*, respectively. $n = 148–334$ cells. *D,* GFP-processing assay in *K. marxianus*. The *K. marxianus* cells used in *B* were grown at 30 °C (*Nut.*) and treated with rapamycin for 1 h (*Rap. 1 h*), and then total lysates were prepared. The samples were subjected to immunoblot analysis using anti-GFP antibody, anti-ScApe1 antibody (cross-reacted with KmApe1), and streptavidin-HRP as a loading control (biotinylated). *proc.GFP*, *prKmApe1*, and *mKmApe1* indicate the processed form of the GFP moiety, the precursor form of KmApe1, and the mature form of KmApe1, respectively. *CBB*, Coomassie Brilliant Blue. *E,* GFP-processing assay under high temperature conditions. *K. marxianus* cells expressing GFP-KmAtg8 and *S. cerevisiae* cells expressing GFP-ScAtg8 were grown at 30 °C, shifted to 37 or 42 °C, and treated with rapamycin for 1 h. *F, K. marxianus* cells used in *E* were observed by fluorescence microscopy.

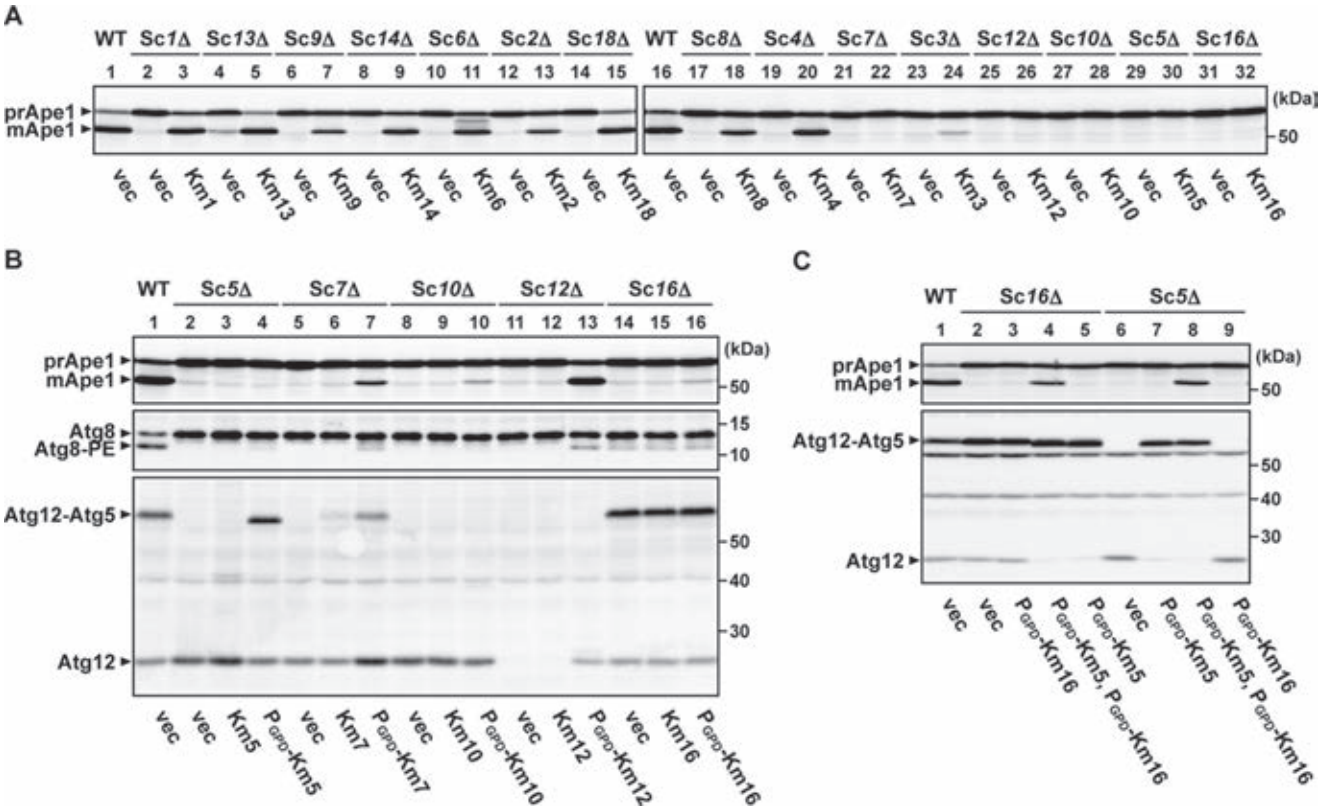


FIGURE 4. **KmAtg proteins complement the functions of ScAtg proteins in *S. cerevisiae*.** *A–C,* complementation analyses of KmAtg proteins in *S. cerevisiae*. KmAtg proteins were expressed in *S. cerevisiae* cells lacking the corresponding Sc*ATG* gene (*Sc*Δ). Each KmAtg protein was expressed under control of its own promoter (*A*) or the Sc*TDH3* ($P_{GPD}$) promoter (*B* and *C*) by using the *CEN* plasmid pRS316. The resultant *S. cerevisiae* cells were grown at 30 °C and treated with rapamycin for 2 h, and then total lysates were prepared. The samples were subjected to immunoblot analysis using anti-ScApe1, anti-ScAtg8, and anti-ScAtg12 antibodies. Atg12-Atg5 indicates not only the ScAtg12-ScAtg5 conjugate, but also the ScAtg12-KmAtg5 heterogeneous conjugate (*B*, *lane 4*). *vec,* vector.

When incubated at 30 °C, both ScAtg8 and KmAtg8 were efficiently conjugated to PE in a time-dependent manner (Fig. 5*B*). However, when ScAtg3 was preincubated at 60 °C, ScAtg8 was not conjugated to PE (Fig. 5*B*, *left panel*), suggesting that ScAtg3 was inactivated by the heat treatment. By contrast, KmAtg3 retained its E2 enzyme activity to some extent even after heat treatment at 60 °C (Fig. 5*B*, *right panel*). These results suggest that KmAtg3 is more thermostable than ScAtg3, consistent with the differences in their $T_m$ values obtained by DSF analysis (Fig. 5*A*).

*KmAtg Proteins Are Highly Soluble Relative to ScAtg Proteins*—To further investigate intrinsic features of KmAtg proteins, we prepared six pairs of ScAtg and KmAtg proteins (Atg3, Atg5, Atg7, Atg8, Atg10, and Atg12, all of which are components of the ubiquitin-like conjugation systems) by using the PURExpress cell-free translation system (GeneFrontier), not containing other intracellular components such as heat shock chaperones. Both ScAtg and KmAtg proteins were efficiently produced; however, ScAtg5, ScAtg7, and ScAtg12 were poorly recovered after high speed centrifugation, suggesting that they aggregated under these conditions (Fig. 5*C*). In contrast to the ScAtg proteins, the KmAtg proteins except for KmAtg7 were efficiently recovered in the supernatant fraction (Fig. 5*C*), implying that the KmAtg proteins used in this assay were more soluble than the corresponding ScAtg proteins.

*KmAtg10 Exhibits a High Resolution NMR Spectrum*—Recently, we reported the solution structure of KmAtg10, determined by NMR spectrometry (29). During our attempt to determine the KmAtg10 structure, we also prepared recombinant ScAtg10; however, the NMR spectrum showed that ScAtg10 was somewhat aggregated and therefore not suitable for structural determination (Fig. 5*D*, *left panel*). By contrast, a high resolution NMR spectrum could be obtained from KmAtg10 (Fig. 5*D*, *right panel*). Sequence alignment between KmAtg10 and ScAtg10 revealed that ScAtg10 contains an extra 13-residue segment located inside the four-stranded β-sheet of the KmAtg10 structure (supplemental Fig. S2*E*). We assumed that the relatively short length of the KmAtg10 sequence might contribute to high resolution of its NMR spectrum (Fig. 5*D*, *right panel*), as well as its improved thermostability as assessed by DSF analysis (Fig. 5*A*), allowing the practical determination of its structure (29). In addition to KmAtg10, we succeeded in determining the structures of other KmAtg proteins, including KmAtg5 (29), the KmAtg18 homolog KmHsv2 (51), the KmAtg7-KmAtg10 complex (30), and the KmAtg1-KmAtg13 complex (52). Taken together with our recent progress in structural biology, these findings indicate that KmAtg proteins, which are more thermostable and soluble than their ScAtg counterparts, are suitable for biochemical and structural studies.

## Discussion

In this study, with the goal of expanding the scope of autophagy research, we demonstrated that the newly isolated thermotolerant yeast strain *K. marxianus* DMKU3-1042 (21) represents a novel experimental system with thermostable Atg

proteins. We first identified a complete set of KmAtg proteins essential for autophagosome formation in *K. marxianus* (Fig. 3), most of which can, at least in part, functionally substitute their counterpart ScAtg proteins in *S. cerevisiae* (Fig. 5). These findings showed that the basal molecular mechanisms underlying autophagosome formation are conserved between these two species. Sequence alignments and bioinformatic analyses showed that most KmAtg proteins are apparently shorter than

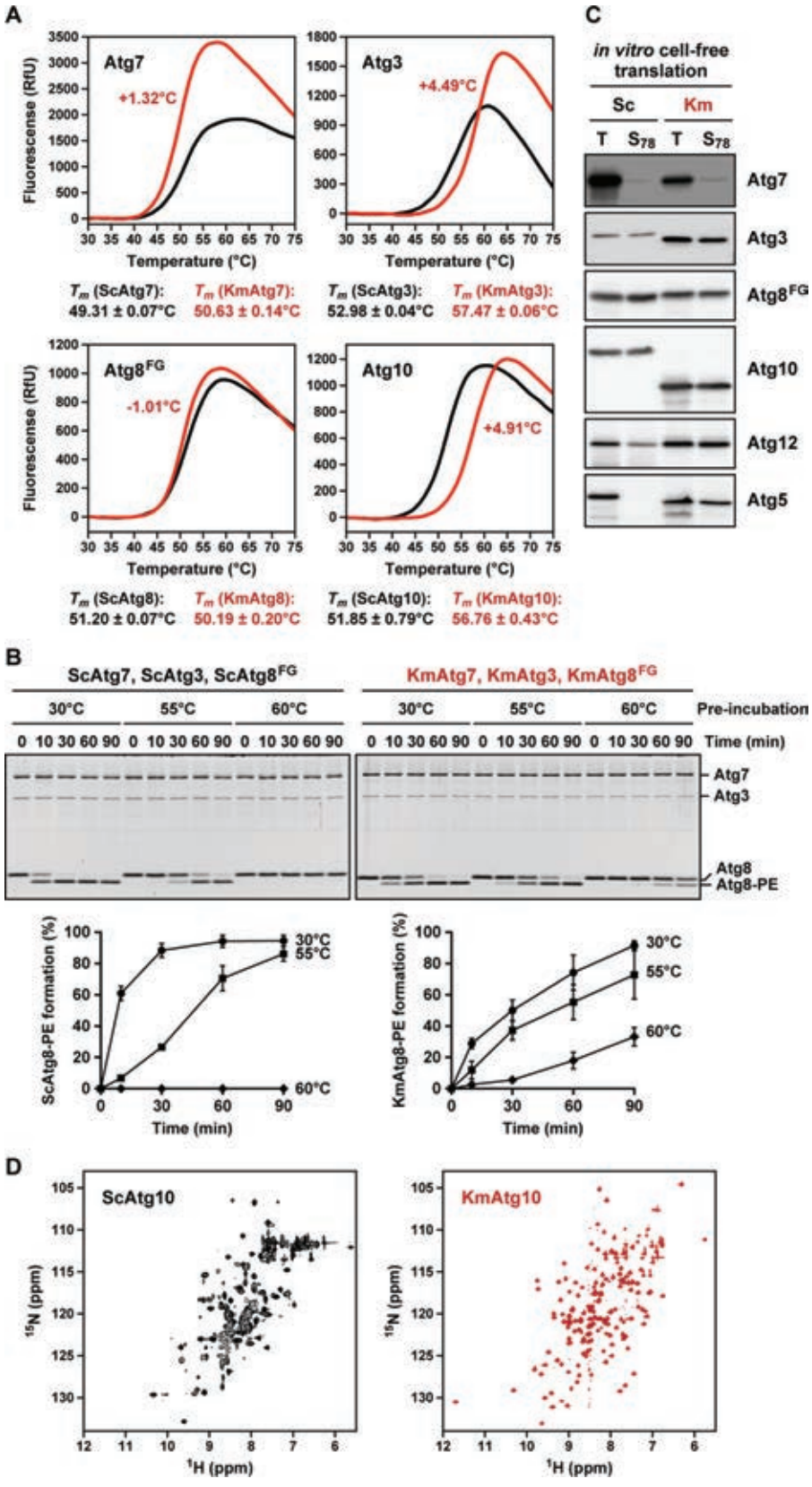

their *S. cerevisiae* counterparts (Fig. 2*A*). Furthermore, Atg proteins are highly diverse between these two species as compared with other proteins (most KmAtg proteins have relatively low identity; located in the *left side* of the *blue box* indicating *Km* < *Sc* in Fig. 1*B*). Our observations suggest that *K. marxianus* will be useful for studies of autophagy. First, similar to *S. cerevisiae* cells, autophagy was efficiently induced in *K. marxianus* cells by nutrient starvation or rapamycin treatment. Second, because the fundamental molecular mechanisms underlying autophagosome formation are conserved between *S. cerevisiae* and *K. marxianus*, the novel insights obtained in *K. marxianus* studies, such as structural information, will be directly applicable to *in vivo* analysis using the well characterized model yeast *S. cerevisiae*, and vice versa. Third, *K. marxianus* cells grow rapidly with doubling times of 45–60 min at 37 °C and reach much higher density than *S. cerevisiae* cells (53), allowing us to perform experiments rapidly and efficiently. Fourth, standard protocols for *K. marxianus* genetics, such as knock-in and knockout techniques, have been established (24, 54, 55). Fifth, autophagy is modestly induced in *K. marxianus* cells even at temperatures above 47 °C.[6] Based on these features, *K. marxianus* is thought to be applicable for studies aimed at elucidating the molecular functions of Atg proteins by *in vitro* analyses, as well as the physiological roles of autophagy *in vivo*, including cellular quality control and stress response to high temperature. In fact, under the high temperature conditions at 37 or 42 °C, while autophagic activity was reduced in *S. cerevisiae* cells, autophagic activity was significantly enhanced in *K. marxianus* cells (Fig. 3*E*).

We also observed some differences between *S. cerevisiae* and *K. marxianus*. Whereas ScAtg11 mostly functions in selective autophagy under nutrient-rich conditions in *S. cerevisiae*, KmAtg11 is required for both selective autophagy and starvation-induced autophagy in *K. marxianus* (Fig. 3*C*). One possible explanation for this is that during evolution, KmAtg11 might have acquired an additional function related to the basal mechanisms of autophagosome formation under starvation conditions. Alternatively, ScAtg11 might have become specific for selective autophagy in *S. cerevisiae* cells. We also found that although either ScAtg11 or ScAtg17 is crucial for PAS formation in *S. cerevisiae* cells (44), PAS assembly of GFP-KmAtg8 was observed even in the absence of the scaffold proteins in *K. marxianus* (Fig. 3*B*, *green bars*, *Kmatg11*Δ *Kmatg17*Δ, *Kmatg11*Δ *Kmatg29*Δ, and *Kmatg11*Δ *Kmatg31*Δ), which was strictly dependent on two ubiquitin-like conjugation systems (Fig. 3*B*, *green bars*, *Kmatg3*Δ, *Kmatg4*Δ, *Kmatg5*Δ, *Kmatg7*Δ, *Kmatg10*Δ, and *Kmatg16*Δ). These observations suggest that in *K. marxianus* cells, GFP-KmAtg8 can assemble to form the PAS-like puncta, irrespective of scaffold proteins such as KmAtg11 and KmAtg17. In mammals, neither Atg11 nor Atg17 is conserved, in which FIP200 plays a key role in the initial step of autophagosome formation (56, 57). The differences between *S. cerevisiae* and *K. marxianus* cells would help us to further understand the common mechanisms underlying the initial step of autophagosome formation, which involves divergent scaffold proteins, including Atg11, Atg17, and FIP200. Alternatively, KmAtg8 could have additional functions other than autophagosome formation in *K. marxianus* cells. We found that even in the absence of the two ubiquitin-like conjugation systems, GFP-KmAtg8 formed several small dots in proximity to the vacuolar membrane (Fig. 3*C*, *gray bars*). A previous study has reported that in *Pichia pastoris* Atg8 is involved in not only autophagy but also in vacuolar membrane dynamics in a lipidation-independent manner (58). KmAtg8 may also have a role in vacuolar morphogenesis or other biological events in a lipidation-independent manner.

From the standpoints of structural and biochemical studies, the most important property of *K. marxianus* is its thermotolerance. Our *in vitro* analyses revealed that several KmAtg proteins have higher thermostability and solubility than ScAtg proteins (Fig. 4), potentially due to their shorter primary sequences (Fig. 2*A*). By using these thermostable recombinant proteins, we have actually succeeded in obtaining structural information about KmAtg1, KmAtg5, KmAtg7, KmAtg10, KmAtg13, and the KmAtg18 homolog KmHsv2 (29, 30, 51, 52). Taken together, our findings clearly indicate that *K. marxianus* has the advantages of thermostability and solubility, making it an especially suitable model organism for structural and biochemical studies. Recently, thermotolerant and thermophilic novel organisms have begun to be used in structural biology. For example, Amlacher *et al.* (20) uncovered molecular details of nuclear pore complexes by using the thermophilic fungus *C. thermophilum*. In the autophagy field, Ragusa *et al.* (59) succeeded in determining the structure of the Atg17-Atg31-Atg29 ternary complex derived from the thermotolerant yeast *Lachancea thermotolerans*. The results of these studies are consistent with the interpretation that thermotolerant or thermophilic organisms are useful for structural and biochemical studies. Currently, structural data about several Atg proteins, such as Atg2, Atg9, Atg11, and Atg14, have not been obtained because of technical difficulty of preparing these proteins. We expect that utilization of *K. marxianus* will help us to obtain structural information about these Atg proteins and will facilitate the elucidation of the molecular mechanisms underlying autophagosome formation.

Our bioinformatic analyses showed that, in addition to the KmAtg proteins, almost half of *K. marxianus* proteins are shorter and more ordered than their *S. cerevisiae* counterparts

FIGURE 5. **KmAtg proteins are more thermostable and soluble than ScAtg proteins.** *A,* KmAtg7, KmAtg3, and KmAtg10 are more thermostable than ScAtg7, ScAtg3, and ScAtg10, respectively. Recombinant Atg proteins (Atg7, Atg3, Atg8$^{FG}$, and Atg10) derived from *K. marxianus* (*red*) and *S. cerevisiae* (*black*) were subjected to DSF analysis. *B,* KmAtg3 is more thermostable than ScAtg3. Recombinant Atg proteins (0.22 $\mu$M Atg7, 0.22 $\mu$M Atg3, and 5 $\mu$M Atg8$^{FG}$) derived from *S. cerevisiae* (*left panel*) and *K. marxianus* (*right panel*) were subjected to *in vitro* PE-conjugation assay (350 mM PE-containing liposome). Before conjugation reaction, ScAtg3 and KmAtg3 were preincubated at 30, 55, or 60 °C for 90 min, and the conjugation reaction was performed at 30 °C for 10, 30, 60, and 90 min. The samples were subjected to urea-containing SDS-PAGE followed by Coomassie Brilliant Blue staining. The PE-conjugated form of Atg8 (Atg8-PE) was quantitated. Total amounts of Atg8 were defined as 100%. *RfU*, relative fluorescence unit. *C,* strep-tagged Atg proteins (Atg7, Atg3, Atg8$^{FG}$, Atg10, Atg12, and Atg5) derived from *K. marxianus* and *S. cerevisiae* were expressed at 37 °C for 4 h by using the PURExpress cell-free translation kit (GeneFrontier). After the translation, the total reaction mixtures (*T*) were centrifuged at 78,000 × *g* for 30 min, and supernatants were prepared ($S_{78}$). The samples were subjected to immunoblot analysis using anti-Strep antibody. *D,* NMR spectra of ScAtg10 (*left panel*) and KmAtg10 (*right panel*).

(Fig. 1). As general features of the *K. marxianus* proteome, the shortened primary sequences and ordered secondary structures may explain the superior thermotolerance of this organism. We hope that utilization of *K. marxianus* will expand the range of structural biology and biochemistry by providing stable recombinant proteins for a multitude of applications.

*Author Contributions*—H. Y. designed the experiments. H. Y., T. S., M. Y., Y. M., H. H., S. K., and C. K. carried out the experiments. H. Y., N. N. N., F. I., T. I., R. A., and Y. O. analyzed and interpreted the data. H. Y. and Y. O. wrote the manuscript. Y. O. supervised the project.

*Acknowledgments—We thank the Bio-Technical Center, Technical Department, Tokyo Institute of Technology for sequencing. We are grateful to the members of the Ohsumi laboratory for materials and helpful discussions.*

**References**


1. Nakatogawa, H., Suzuki, K., Kamada, Y., and Ohsumi, Y. (2009) Dynamics and diversity in autophagy mechanisms: lessons from yeast. *Nat. Rev. Mol. Cell Biol.* **10,** 458–467
2. Mizushima, N., Yoshimori, T., and Ohsumi, Y. (2011) The role of Atg proteins in autophagosome formation. *Annu. Rev. Cell Dev. Biol.* **27,** 107–132
3. Ohsumi, Y. (2014) Historical landmarks of autophagy research. *Cell Res.* **24,** 9–23
4. Feng, Y., He, D., Yao, Z., and Klionsky, D. J. (2014) The machinery of macroautophagy. *Cell Res.* **24,** 24–41
5. Mizushima, N., and Komatsu, M. (2011) Autophagy: renovation of cells and tissues. *Cell* **147,** 728–741
6. Levine, B., Mizushima, N., and Virgin, H. W. (2011) Autophagy in immunity and inflammation. *Nature* **469,** 323–335
7. Rubinsztein, D. C., Codogno, P., and Levine, B. (2012) Autophagy modulation as a potential therapeutic target for diverse diseases. *Nat. Rev. Drug Discov.* **11,** 709–730
8. Tsukada, M., and Ohsumi, Y. (1993) Isolation and characterization of autophagy-defective mutants of *Saccharomyces cerevisiae*. *FEBS Lett.* **333,** 169–174
9. Matsushita, M., Suzuki, N. N., Obara, K., Fujioka, Y., Ohsumi, Y., and Inagaki, F. (2007) Structure of Atg5-Atg16, a complex essential for autophagy. *J. Biol. Chem.* **282,** 6763–6772
10. Yamada, Y., Suzuki, N. N., Hanada, T., Ichimura, Y., Kumeta, H., Fujioka, Y., Ohsumi, Y., and Inagaki, F. (2007) The crystal structure of Atg3, an autophagy-related ubiquitin carrier protein (E2) enzyme that mediates Atg8 lipidation. *J. Biol. Chem.* **282,** 8036–8043
11. Fujioka, Y., Noda, N. N., Nakatogawa, H., Ohsumi, Y., and Inagaki, F. (2010) Dimeric coiled-coil structure of *Saccharomyces cerevisiae* Atg16 and its functional significance in autophagy. *J. Biol. Chem.* **285,** 1508–1515
12. Yamaguchi, M., Noda, N. N., Nakatogawa, H., Kumeta, H., Ohsumi, Y., and Inagaki, F. (2010) Autophagy-related protein 8 (Atg8) family interacting motif in Atg3 mediates the Atg3-Atg8 interaction and is crucial for the cytoplasm-to-vacuole targeting pathway. *J. Biol. Chem.* **285,** 29599–29607
13. Hong, S. B., Kim, B. W., Lee, K. E., Kim, S. W., Jeon, H., Kim, J., and Song, H. K. (2011) Insights into noncanonical E1 enzyme activation from the structure of autophagic E1 Atg7 with Atg8. *Nat. Struct. Mol. Biol.* **18,** 1323–1330
14. Taherbhoy, A. M., Tait, S. W., Kaiser, S. E., Williams, A. H., Deng, A., Nourse, A., Hammel, M., Kurinov, I., Rock, C. O., Green, D. R., and Schulman, B. A. (2011) Atg8 transfer from Atg7 to Atg3: a distinctive E1-E2 architecture and mechanism in the autophagy pathway. *Mol. Cell* **44,** 451–461
15. Noda, N. N., Satoo, K., Fujioka, Y., Kumeta, H., Ogura, K., Nakatogawa, H., Ohsumi, Y., and Inagaki, F. (2011) Structural basis of Atg8 activation by a homodimeric E1, Atg7. *Mol. Cell* **44,** 462–475
16. Ichimura, Y., Imamura, Y., Emoto, K., Umeda, M., Noda, T., and Ohsumi, Y. (2004) *In vivo* and *in vitro* reconstitution of Atg8 conjugation essential for autophagy. *J. Biol. Chem.* **279,** 40584–40592
17. Nakatogawa, H., Ichimura, Y., and Ohsumi, Y. (2007) Atg8, a ubiquitin-like protein required for autophagosome formation, mediates membrane tethering and hemifusion. *Cell* **130,** 165–178
18. Hanada, T., Noda, N. N., Satomi, Y., Ichimura, Y., Fujioka, Y., Takao, T., Inagaki, F., and Ohsumi, Y. (2007) The Atg12-Atg5 conjugate has a novel E3-like activity for protein lipidation in autophagy. *J. Biol. Chem.* **282,** 37298–37302
19. Chien, A., Edgar, D. B., and Trela, J. M. (1976) Deoxyribonucleic acid polymerase from the extreme thermophile *Thermus aquaticus*. *J. Bacteriol.* **127,** 1550–1557
20. Amlacher, S., Sarges, P., Flemming, D., van Noort, V., Kunze, R., Devos, D. P., Arumugam, M., Bork, P., and Hurt, E. (2011) Insight into structure and assembly of the nuclear pore complex by utilizing the genome of a eukaryotic thermophile. *Cell* **146,** 277–289
21. Limtong, S., Sringiew, C., and Yongmanitchai, W. (2007) Production of fuel ethanol at high temperature from sugar cane juice by a newly isolated *Kluyveromyces marxianus*. *Bioresour. Technol.* **98,** 3367–3374
22. Kaiser, C., Michaelis, S., and Mitchell, A. (1994) *Methods in Yeast Genetics.* Cold Spring Harbor Laboratory Press, Cold Spring Harbor, NY
23. Janke, C., Magiera, M. M., Rathfelder, N., Taxis, C., Reber, S., Maekawa, H., Moreno-Borchart, A., Doenges, G., Schwob, E., Schiebel, E., and Knop, M. (2004) A versatile toolbox for PCR-based tagging of yeast genes: new fluorescent proteins, more markers and promoter substitution cassettes. *Yeast* **21,** 947–962
24. Abdel-Banat, B. M., Nonklang, S., Hoshida, H., and Akada, R. (2010) Random and targeted gene integrations through the control of non-homologous end joining in the yeast *Kluyveromyces marxianus*. *Yeast* **27,** 29–39
25. Sikorski, R. S., and Hieter, P. (1989) A system of shuttle vectors and yeast host strains designed for efficient manipulation of DNA in *Saccharomyces cerevisiae*. *Genetics* **122,** 19–27
26. Yamamoto, H., Kakuta, S., Watanabe, T. M., Kitamura, A., Sekito, T., Kondo-Kakuta, C., Ichikawa, R., Kinjo, M., and Ohsumi, Y. (2012) Atg9 vesicles are an important membrane source during early steps of autophagosome formation. *J. Cell Biol.* **198,** 219–233
27. Tokunaga, M., Imamoto, N., and Sakata-Sogawa, K. (2008) Highly inclined thin illumination enables clear single-molecule imaging in cells. *Nat. Methods* **5,** 159–161
28. Yamaguti, M., Suzuki, N. N., Fujioka, Y., Ohsumi, Y., and Inagaki, F. (2007) Crystallization and preliminary x-ray analysis of Atg10. *Acta Crystallogr. Sect. F. Struct. Biol. Cryst. Commun.* **63,** 443–445
29. Yamaguchi, M., Noda, N. N., Yamamoto, H., Shima, T., Kumeta, H., Kobashigawa, Y., Akada, R., Ohsumi, Y., and Inagaki, F. (2012) Structural insights into Atg10-mediated formation of the autophagy-essential Atg12-Atg5 conjugate. *Structure* **20,** 1244–1254
30. Yamaguchi, M., Matoba, K., Sawada, R., Fujioka, Y., Nakatogawa, H., Yamamoto, H., Kobashigawa, Y., Hoshida, H., Akada, R., Ohsumi, Y., Noda, N. N., and Inagaki, F. (2012) Noncanonical recognition and UBL loading of distinct E2s by autophagy-essential Atg7. *Nat. Struct. Mol. Biol.* **19,** 1250–1256
31. Niesen, F. H., Berglund, H., and Vedadi, M. (2007) The use of differential scanning fluorimetry to detect ligand interactions that promote protein stability. *Nat. Protoc.* **2,** 2212–22121
32. Delaglio, F., Grzesiek, S., Vuister, G. W., Zhu, G., Pfeifer, J., and Bax, A. (1995) NMRPipe: a multidimensional spectral processing system based on UNIX pipes. *J. Biomol. NMR* **6,** 277–293
33. Kneller, D. G., and Goddard, T. D. (1997) *SPARKY,* Version 3.105. University of California, San Francisco
34. Lertwattanasakul, N., Kosaka, T., Hosoyama, A., Suzuki, Y., Rodrussamee, N., Matsutani, M., Murata, M., Fujimoto, N., Suprayogi, Tsuchikane, K., Limtong, S., Fujita, N., and Yamada, M. (2015) Genetic basis of the highly efficient yeast *Kluyveromyces marxianus*: complete genome sequence and transcriptome analyses. *Biotechnol. Biofuels* **8,** 47
35. Prilusky, J., Felder, C. E., Zeev-Ben-Mordehai, T., Rydberg, E. H., Man, O.,

Beckmann, J. S., Silman, I., and Sussman, J. L. (2005) FoldIndex: a simple tool to predict whether a given protein sequence is intrinsically unfolded. *Bioinformatics* **21,** 3435–3438
36. Takeshige, K., Baba, M., Tsuboi, S., Noda, T., and Ohsumi, Y. (1992) Autophagy in yeast demonstrated with proteinase-deficient mutants and conditions for its induction. *J. Cell Biol.* **119,** 301–311
37. Kirisako, T., Baba, M., Ishihara, N., Miyazawa, K., Ohsumi, M., Yoshimori, T., Noda, T., and Ohsumi, Y. (1999) Formation process of autophagosome is traced with Apg8/Aut7p in yeast. *J. Cell Biol.* **147,** 435–446
38. Kabeya, Y., Mizushima, N., Ueno, T., Yamamoto, A., Kirisako, T., Noda, T., Kominami, E., Ohsumi, Y., and Yoshimori, T. (2000) LC3, a mammalian homologue of yeast Apg8p, is localized in autophagosome membranes after processing. *EMBO J.* **19,** 5720–5728
39. Noda, T., Matsuura, A., Wada, Y., and Ohsumi, Y. (1995) Novel system for monitoring autophagy in the yeast *Saccharomyces cerevisiae*. *Biochem. Biophys. Res. Commun.* **210,** 126–132
40. Kirisako, T., Ichimura, Y., Okada, H., Kabeya, Y., Mizushima, N., Yoshimori, T., Ohsumi, M., Takao, T., Noda, T., and Ohsumi, Y. (2000) The reversible modification regulates the membrane-binding state of Apg8/Aut7 essential for autophagy and the cytoplasm to vacuole targeting pathway. *J. Cell Biol.* **151,** 263–276
41. Ichimura, Y., Kirisako, T., Takao, T., Satomi, Y., Shimonishi, Y., Ishihara, N., Mizushima, N., Tanida, I., Kominami, E., Ohsumi, M., Noda, T., and Ohsumi, Y. (2000) A ubiquitin-like system mediates protein lipidation. *Nature* **408,** 488–492
42. Shintani, T., and Klionsky, D. J. (2004) Cargo proteins facilitate the formation of transport vesicles in the cytoplasm to vacuole targeting pathway. *J. Biol. Chem.* **279,** 29889–29894
43. Suzuki, K., Kirisako, T., Kamada, Y., Mizushima, N., Noda, T., and Ohsumi, Y. (2001) The pre-autophagosomal structure organized by concerted functions of APG genes is essential for autophagosome formation. *EMBO J.* **20,** 5971–5981
44. Suzuki, K., Kubota, Y., Sekito, T., and Ohsumi, Y. (2007) Hierarchy of Atg proteins in pre-autophagosomal structure organization. *Genes Cells* **12,** 209–218
45. Kabeya, Y., Noda, N. N., Fujioka, Y., Suzuki, K., Inagaki, F., and Ohsumi, Y. (2009) Characterization of the Atg17-Atg29-Atg31 complex specifically required for starvation-induced autophagy in *Saccharomyces cerevisiae*. *Biochem. Biophys. Res. Commun.* **389,** 612–615
46. Klionsky, D. J., Cueva, R., and Yaver, D. S. (1992) Aminopeptidase I of *Saccharomyces cerevisiae* is localized to the vacuole independent of the secretory pathway. *J. Cell Biol.* **119,** 287–299
47. Scott, S. V., Hefner-Gravink, A., Morano, K. A., Noda, T., Ohsumi, Y., and Klionsky, D. J. (1996) Cytoplasm-to-vacuole targeting and autophagy employ the same machinery to deliver proteins to the yeast vacuole. *Proc. Natl. Acad. Sci. U.S.A.* **93,** 12304–12308
48. Mizushima, N., Noda, T., Yoshimori, T., Tanaka, Y., Ishii, T., George, M. D., Klionsky, D. J., Ohsumi, M., and Ohsumi, Y. (1998) A protein conjugation system essential for autophagy. *Nature* **395,** 395–398
49. Mizushima, N., Noda, T., and Ohsumi, Y. (1999) Apg16p is required for the function of the Apg12p-Apg5p conjugate in the yeast autophagy pathway. *EMBO J.* **18,** 3888–3896
50. Kuma, A., Mizushima, N., Ishihara, N., and Ohsumi, Y. (2002) Formation of the approximately 350-kDa Apg12-Apg5.Apg16 multimeric complex, mediated by Apg16 oligomerization, is essential for autophagy in yeast. *J. Biol. Chem.* **277,** 18619–18625
51. Watanabe, Y., Kobayashi, T., Yamamoto, H., Hoshida, H., Akada, R., Inagaki, F., Ohsumi, Y., and Noda, N. N. (2012) Structure-based analyses reveal distinct binding sites for Atg2 and phosphoinositides in Atg18. *J. Biol. Chem.* **287,** 31681–31690
52. Fujioka, Y., Suzuki, S. W., Yamamoto, H., Kondo-Kakuta, C., Kimura, Y., Hirano, H., Akada, R., Inagaki, F., Ohsumi, Y., and Noda, N. N. (2014) Structural basis of starvation-induced assembly of the autophagy initiation complex. *Nat. Struct. Mol. Biol.* **21,** 513–521
53. Fonseca, G. G., Heinzle, E., Wittmann, C., and Gombert, A. K. (2008) The yeast *Kluyveromyces marxianus* and its biotechnological potential. *Appl. Microbiol. Biotechnol.* **79,** 339–354
54. Yarimizu, T., Nonklang, S., Nakamura, J., Tokuda, S., Nakagawa, T., Lorreungsil, S., Sutthikhumpha, S., Pukahuta, C., Kitagawa, T., Nakamura, M., Cha-Aim, K., Limtong, S., Hoshida, H., and Akada, R. (2013) Identification of auxotrophic mutants of the yeast *Kluyveromyces marxianus* by non-homologous end joining-mediated integrative transformation with genes from *Saccharomyces cerevisiae*. *Yeast* **30,** 485–500
55. Hoshida, H., Murakami, N., Suzuki, A., Tamura, R., Asakawa, J., Abdel-Banat, B. M., Nonklang, S., Nakamura, M., and Akada, R. (2014) Non-homologous end joining-mediated functional marker selection for DNA cloning in the yeast *Kluyveromyces marxianus*. *Yeast* **31,** 29–46
56. Hara, T., Takamura, A., Kishi, C., Iemura, S., Natsume, T., Guan, J. L., and Mizushima, N. (2008) FIP200, a ULK-interacting protein, is required for autophagosome formation in mammalian cells. *J. Cell Biol.* **181,** 497–510
57. Hara, T., and Mizushima, N. (2009) Role of ULK-FIP200 complex in mammalian autophagy: FIP200, a counterpart of yeast Atg17? *Autophagy* **5,** 85–87
58. Tamura, N., Oku, M., and Sakai, Y. (2010) Atg8 regulates vacuolar membrane dynamics in a lipidation-independent manner in *Pichia pastoris*. *J. Cell Sci.* **123,** 4107–4116
59. Ragusa, M. J., Stanley, R. E., and Hurley, J. H. (2012) Architecture of the Atg17 complex as a scaffold for autophagosome biogenesis. *Cell* **151,** 1501–1512